



RESEARCH AND DEVELOPMENT TECHNICAL REPORT

ECOM-0239-1

OPTICAL PUMPS FOR LASERS

TRI-ANNUAL REPORT No. 1

By

LOWELL NOBLE AND C. B. KRETSCHMER

MARCH, 1972

DISTRIBUTION STATEMENT

Approved for public release; distribution unlimited.

AD 742734

ECOM

UNITED STATES ARMY ELECTRONICS COMMAND · FORT MONMOUTH, N.J. 07703

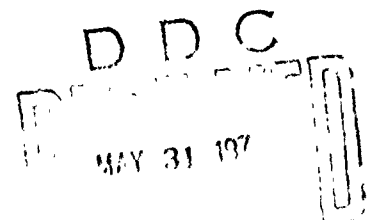
CONTRACT DAAB07-71-C-0239

ILC, INCORPORATED

SUNNYVALE, CALIFORNIA 94086

R-ILC-71-30

Reproduced by  
NATIONAL TECHNICAL  
INFORMATION SERVICE  
Springfield, Va 22151



## NOTICES

### Disclaimers

The findings in this report are not to be construed as an official Department of the Army position unless so designated by other authorized documents.

The citation of trade names and names of manufacturers in this report is not to be construed as official Government endorsement or approval of commercial products or services referenced herein.

### Disposition

Destroy this report when it is no longer needed. Do not return it to the originator.

ACCESSION NO.	
DTIC	WRITE SECTION <input checked="" type="checkbox"/>
OSC	SUPP SECTION <input type="checkbox"/>
REFERENCES	<input type="checkbox"/>
JUSTIFICATION	
BY	
DISTRIBUTION AVAILABILITY STATEMENT	
REST.	AVAIL. STATEMENT
A	

TR ECOM-0239-1  
MARCH 1972

REPORTS CONTROL SYMBOL  
OSD-1366

OPTICAL PUMPS FOR LASERS

TRIENNIAL REPORT NO. 1  
17 May 1971 to 17 September 1971

CONTRACT NO. DAAB07-71-C-0239  
DA Project No. 1H6-62705-A-055-02-68

DISTRIBUTION STATEMENT

Approved for public release; distribution unlimited.

By

Lowell Noble and C.B. Kretschmer

ILC, INC.  
Sunnyvale, California 94086

For

U. S. ARMY ELECTRONICS COMMAND, FORT MONMOUTH, N. J. 07703

Unclassified

Security Classification

DOCUMENT CONTROL DATA - R & D

(Security classification of title, body of abstract and indexing annotation must be entered when the overall report is classified)

1. ORIGINATING ACTIVITY (Corporate author) ILC, INC. 164 Commercial Street Sun. yvale, California	2a. REPORT SECURITY CLASSIFICATION Unclassified
	2b. GROUP

3. REPORT TITLE  
OPTICAL PUMPS FOR LASERS

4. DESCRIPTIVE NOTES (Type of report and inclusive dates)  
Triannual Report No. 1, 17 May 1971 to 17 September 1971

5. AUTHOR(S) (First name, middle initial, last name)  
Lowell Noble

6. REPORT DATE March 1972	7a. TOTAL NO. OF PAGES 58	7b. NO. OF REFS 7
------------------------------	------------------------------	----------------------

8a. CONTRACT OR GRANT NO. DAAB07-71-C-0239	9a. ORIGINATOR'S REPORT NUMBER(S) ECOM-0239-1
b. PROJECT NO.	
c.	9b. OTHER REPORT NO(S) (Any other numbers that may be assigned this report)
d.	

10. DISTRIBUTION STATEMENT  
Approved for public release; distribution unlimited

11. SUPPLEMENTARY NOTES	12. SPONSORING MILITARY ACTIVITY U.S. Army Electronics Command Fort Monmouth, New Jersey 07703 Attn: AMSEL-TL-BG
-------------------------	---

13. ABSTRACT  
 → The objective of this program is to increase both the output efficiency and the reproducibility of optical pumps for Nd:YAG lasers. This report covers the work carried out during the first four months of the program.

→ Lamps with quartz envelopes doped with cerium, which converts ultra violet radiation to visible radiation, have been tested and found to emit 15% more light in the region between 0.4 and 0.65  $\mu$ m than lamps made of undoped quartz.

An analysis was made of the externally triggered mode and simmer mode of flashlamp operation. It is hypothesized that the lower electron temperature and the lower current density achieved in simmer mode operation are responsible for the enhanced light output obtained in the simmer mode.

→ A technique was devised to measure lamp arc growth during a pulse. A lamp of 4 mm bore diameter and 2.125 inch arc length, filled with 450 Torr of xenon, required a 20 joule pulse to fill the bore within a 100  $\mu$ s period.

Lamps have been manufactured to tolerances significantly tighter than normal; they may provide more reproducible light output than is provided by standard lamps.

14. KEY WORDS	LINK A		LINK B		LINK C	
	ROLE	WT	ROLE	WT	ROLE	WT
Optical Pumps Flash Lamps Inert Gas Lamps Lasers Laser Pumping						

## TABLE OF CONTENTS

	<u>Page No.</u>
FOREWORD	i
ABSTRACT	ii
LIST OF ILLUSTRATIONS	iii
LIST OF TABLES	v
1.0 SUMMARY AND CONCLUSIONS	1
2.0 INTRODUCTION	3
2.1 Objectives	3
2.2 Approach	3
3.0 BACKGROUND	6
4.0 IMPROVING LASER OPERATING EFFICIENCY	14
4.1 Lamps with Cerium Doped Quartz Envelopes	14
4.2 Operation of Lamps in Simmer Mode	15
4.3 Triggering Improvements	16
5.0 IMPROVING LASER OPERATING REPRODUCIBILITY	18
5.1 Analysis of Lamp Variables	18
5.2 Fluorescence Analysis Instrumentation	21
5.3 Lamp Fabrication	23
5.4 Life Test Instrumentation	24
6.0 REFERENCES	25

## FOREWORD

The work reported herein was accomplished under Contract Number DAAB07-71-C-0239 for the Gaseous Electron Devices Team, Beam and Plasma Device Technical Area of the Electronic Technology and Devices Laboratory under the guidance of Mr. Norman Yeamans, the contracting officer's designated representative.

The studies being carried out on this program are being performed in the Engineering Division of ILC, which is under the direction of Dr. L. Reed. Martin Marietta is responsible for the laser effort on a sub-contract basis.

Mr. Lowell Noble is the principal investigator. Dr. Carl Kretschmer developed the theory of simmer mode operation. Mr. B. Maynard and Mr. Harry Flentz are carrying out the optical measurements and data reduction. Mr. D. Alexander is responsible for flashlamp fabrication. Mr. D. Allen is responsible for the auxiliary digitizing modification to the fluorescent analysis instrument and Mr. M. Crasis designed the multiple lamp life testing unit.

Mr. P. M. Rushworth of Martin Marietta is responsible for laser testing.

## ABSTRACT

The objective of this program is to increase both the output efficiency and the reproducibility of optical pumps for Nd:YAG lasers. This report covers the work carried out during the first four months of the program.

Lamps with quartz envelopes doped with cerium, which converts ultra violet radiation to visible radiation, have been tested and found to emit 15% more light in the region between 0.4 and 0.65 $\mu$  than lamps made of undoped quartz.

An analysis was made of the externally triggered mode and simmer mode of flashlamp operation. It is hypothesized that the lower electron temperature and the lower current density achieved in simmer mode operation are responsible for the enhanced light output obtained in the simmer mode.

A technique was devised to measure lamp arc growth during a pulse. A lamp of 4 mm bore diameter and 2.125 inch arc length, filled with 450 Torr of xenon, required a 20 joule pulse to fill the bore within a 100 $\mu$ s period.

Lamps have been manufactured to tolerances significantly tighter than normal; they may provide more reproducible light output than is provided by standard lamps.

## LIST OF ILLUSTRATIONS

- FIGURE 1 LASER OUTPUT DATA FOR 3000 TORR KRYPTON LAMP AND 450 TORR XENON LAMP
- FIGURE 2 LASER OUTPUT DATA FOR XENON LAMP FOR SIMMER PULSE AND EXTERNAL TRIGGER OPERATION
- FIGURE 3 COMPARATIVE SPECTRAL DATA FOR A CERIUM DOPED QUARTZ ENVELOPE LAMP AND A STANDARD QUARTZ ENVELOPE LAMP
- FIGURE 4 EXCITATION SPECTRUM FOR Nd:YAG
- FIGURE 5 FOV DATA FOR 1500 TORR - XENON LAMPS, EXTERNAL TRIGGER AND SIMMER PULSE (10 JOULES)
- FIGURE 6 GROTRIAN ENERGY LEVEL DIAGRAM FOR KRYPTON
- FIGURE 7 BLOCK DIAGRAM OF PULSE ARC GROWTH IMAGE RECORDER
- FIGURE 8 PULSE ARC GROWTH IMAGE RECORDER
- FIGURE 9 CURRENT-TIME CURVES AND PHOTOGRAPHS OF PLASMA FOR PULSE ENERGIES OF 5, 10, 20, 40 AND 60 JOULES
- FIGURE 10 PLASMA DIAMETER AS A FUNCTION OF INPUT ENERGY
- FIGURE 11 PLASMA GROWTH IN L349 AT 5 JOULES
- FIGURE 12 PLASMA GROWTH IN L349 AT 10 JOULES
- FIGURE 13 PLASMA GROWTH IN L349A AT 5 JOULES
- FIGURE 14 PLASMA GROWTH IN L349A AT 10 JOULES
- FIGURE 15 PLASMA GROWTH IN L349A AT 10 JOULES NEAR CATHODE
- FIGURE 16 PLASMA DIAMETER IN L349 AT 5 JOULES

List of Illustrations - Continued

- FIGURE 17 PLASMA DIAMETER IN L349A AT 5 JOULES
- FIGURE 18 PLASMA DIAMETER IN L349 AT 10 JOULES
- FIGURE 19 PLASMA DIAMETER IN L349A AT 10 JOULES
- FIGURE 20 SCHEMATIC DIAGRAM OF PULSED FLUORESCENT ANALYSIS TESTER WITH DIGITAL READOUT ATTACHMENT
- FIGURE 21 PHOTOGRAPH OF PULSED FLUORESCENT ANALYSIS TESTER WITH DIGITAL READOUT ATTACHMENT
- FIGURE 22 BORE SIZE DISTRIBUTION ON 4 X 6 MM AMERSIL QUARTZ TUBING, FREQUENCY BAR CHART
- FIGURE 23 BORE SIZE DISTRIBUTION ON GERMISIL QUARTZ TUBING, FREQUENCY POLYGON

LIST OF TABLES

		<u>Page No.</u>
TABLE I	Nd:YAG LASER PROGRAM GOALS	4
TABLE II	IMPROVEMENTS IN LAMP USEFUL LIGHT OUTPUT AND LASER OUTPUT	8
TABLE III	OPTIMIZED FLASHLAMP-CIRCUIT PARAMETERS FOR THE MOST EFFICIENT LAMP DEVELOPED ON THE PRIOR PROGRAM	13
TABLE IV	MODE I OPERATION - OPTIMIZED FLASHLAMP CIRCUIT PARAMETERS	19
TABLE V	MODE II OPERATION - OPTIMIZED FLASHLAMP CIRCUIT PARAMETERS	20
TABLE VI	OBSERVED VARIATIONS REQUIRED TO ASSURE (WITH 90% CONFIDENCE) THAT 99.7% OF POPULATION LIES WITHIN $\pm 5\%$	21
TABLE VII	REPLICATE FOV DATA FOR A SINGLE LAMP	22

## 1.0 SUMMARY AND CONCLUSIONS

Work is being carried out to increase the overall efficiency (to 4%) and reproducibility (to  $\pm 5\%$ ) of a pulsed Nd:YAG laser that uses a 1/4 inch by 2-1/2 inch laser rod and a 10 joule pump lamp. These results will then be applied to improving the overall efficiency and reproducibility of a laser that uses a 3 mm x 30 mm Nd:YAG laser rod and a 5 joule pump lamp. This performance is to be attained by improving lamps, their associated electronics and the related laser cavities. The best comparable laser efficiency previously achieved was 2.32%.<sup>(1)</sup> That laser was pumped with a 10 joule flashlamp of 2.125 inch arc length, 3 mm bore, filled with krypton to 1500 Torr. The flash duration was 80 microseconds.

The circuit analysis presently used for determining the L, C and V parameters of a single mesh flashlamp pulsing network assumes an arc that fills the bore. With more precision the arc growth may be described by an equation of the form

$$d_a = k \cdot l \cdot \frac{i^n}{v}$$

where  $d_a$  is the varying arc diameter of length  $l$  through which a current passes with a voltage drop  $v$ ;  $k$  and  $n$  are constants, which can be determined experimentally. This equation is being used as a starting point to develop a more precise circuit analysis for flashlamp driving circuits for the case of a partially filled bore.

The values of  $d_a$  throughout a  $100\mu$ s pulse have been measured in 4 mm bore, 2.125 inch arc length, 450 Torr xenon flashlamps pulsed at 5 to 60 joules. An external trigger wire was used. A newly developed image intensifier photographic technique was applied to photograph the plasma and measure  $d_a$ . (The bore of the flashtube is found to be filled only with input energies above 20 joules.)

The normally erratic growth of the arc has been changed to a smooth radial arc growth by placing a thin metallic strip along the side of the flash tube for triggering. This improvement is expected to allow better imaging of the arc onto the laser rod.

Flashtubes with envelopes of cerium-doped quartz have been shown

to produce 15% more light output in the 0.4 to 0.65 $\mu$ m wavelength band compared to normal quartz envelope lamps, by down converting the UV energy of the arc.

Comparison of the externally triggered mode and the simmer mode of lamp initiation has shown that the increase in light output obtained with the simmer mode results from enhancement of line radiation (which is in the Nd:YAG pump band) and depression of continuum radiation, compared to that obtained with standard triggering. This phenomenon, it is hypothesized, results from both lower electron temperatures and lower current densities.

The main fabrication variation affecting the reproducibility of lamp output is variation in the bore diameter of the lamp. 4mm bore lamps were produced with bore diameter variations of only  $\pm 0.05$  mm.

In order to increase the reproducibility of light output, digital read-out equipment has been constructed to measure the radiation in the excitation bands of Nd:YAG. The digital read-out replaces the less accurate oscilloscope procedures used previously. (1) A five-position station has been constructed for measuring the reproducibility of these lamps as they age.

The inferences that may be drawn from the work performed so far are:

1. Laser lamps with cerium-doped-quartz envelopes produce more radiation in the 0.4 to 0.65 $\mu$  region than lamps with clear fused quartz envelopes. Laser output efficiencies will probably be increased through pumping of the 0.58 $\mu$  band.
2. Lamps with a metal stripe trigger wire produce more uniform discharges than lamps without the stripe and probably increase laser efficiency through improved imaging in the rod.
3. Improvements in lamp efficiency have been achieved using the simmer mode of lamp operation, which, it is suggested, modifies arc initiation processes to decrease electron temperature and to decrease current density.
4. Measurements of plasma diameter during arc growth have been made that show that bores of 4mm lamps are not filled during 5 and 10 joule pulsing. Improvements in

designing flashlamp driving circuits specifically for unfilled bore lamps may increase the pumping efficiency.

5. Instrumentation has been developed with which the reproducibility (of the output within the Nd:YAG pumping bands) of a single lamp was found within 10 pulses to vary an average of 0.7% and a maximum of 1.4% of the mean value. How much of the measured variation are due to the lamp and how much to the instrumentation is not yet known.

## 2.0 INTRODUCTION

The purpose of this program is to increase both the efficiency and the reproducibility of Nd:YAG lasers through improvements in lamps, the their associated power supplies, and in laser cavities. This work follows a previous contract, (1) which was initiated to improve the performance of lightweight manportable laser illuminators and target designators.

### 2.1 Objectives

Improved laser performance is sought for two types of laser operating modes, each of which requires the development of a distinctly different pump lamp. A feasibility study of "Optical Pumps for Holmium Lasers" was substituted for a third mode of operation. Table I gives the specifications and performance goals for the two modes of operation.

### 2.2 Approach

The execution of this program is divided into two tasks. The first task is to increase laser output efficiency and, if necessary, lamp life. The second task is to determine the reproducibility of lamp and laser output before and during life tests and, if necessary, improve lamp reproducibility.

TABLE I  
Nd:YAG LASER PROGRAM GOALS

	<u>Mode I</u>	<u>Mode II</u>
<u>Operating Conditions</u>		
Energy Input (joules)	5	10
Repetition Rate (pps)	1	20
<u>Dimensional Constraints</u>		
Laser Rod OD (mm)	3	6
Laser Rod Length (mm)	30	63.5
Lamp Overall Length (mm)	63.5	open
<u>Performance Objectives</u>		
Lamp Life (pulses)*	$10^6$	$10^7$
Initial Lamp-to-Lamp Reproducibility (Laser Output)	$\pm 5\%$	$\pm 5\%$
Overall Laser Efficiency	2.5%	4%
Cooling	None	Liquid

\*Laser life is defined as the number of pulses at which the output has dropped by 20% of its initial value.

The approach to increasing laser efficiency involves:

1. Obtaining a more detailed understanding of the plasma discharge process in the pump lamp.
2. Incorporating new envelope materials, fabrication processes and trigger wire fabrication techniques into the manufacture of lamps. Each may incrementally add to pump lamp efficiency.
3. Improving the energy delivery from the PFN (pulse forming network) by:
  - a) Improving PFN-to-lamp matching design techniques that are applicable when the arc does not fill the bore.
  - b) Developing new matching circuits.
4. Modifying the laser cavity designs to accept:
  - a) the new lamps
  - b) new triggering techniques
  - c) other cavity improvements.

The second task, lamp reproducibility, requires very precise measurements of lamp light output. Such measurements require improvements in existing instrumentation.

The reproducibility of laser output may be improved by:

- 1) Using lamp materials that are manufactured to closer dimensional tolerances.
- 2) Maintaining a close control over the gas filling and other manufacturing processes.

- 3) Introducing new triggering methods, power supply concepts and laser cavity changes that can improve reproducibility.

The laser output measurements are being made principally by Martin-Marietta. Additional laser output measurements are also being made in cooperation with other laser manufacturers. The amount of expensive in-laser testing required is reduced by the use of a recently developed instrument that directly measures the "useful" light that a pump lamp emits, i.e., the light that can be used to pump the excitation bands of the Nd:YAG laser. (1) This device is called a differential fluorescence analysis instrument, and the useful light output is measured in terms of a fluorescent output voltage (FOV). The useful light output must be measured with a high degree of precision in order to determine the lamp-to-lamp light output reproducibility. Consequently the existing differential fluorescence analysis instrument is being improved to provide greater precision.

A statistical approach to the measurement of lamp light output reproducibility is being undertaken. Flash lamp life test equipment, capable of testing five lamps at a time, has been constructed for this purpose.

### 3.0 BACKGROUND

Work carried out under a previous optical pump contract<sup>(1)</sup> resulted in the efficiency improvements shown in Table II and Figure 1. The baseline for the efficiency comparisons was the performance of the standard lamp employed for target designator and illumination applications prior to this investigation: a 450 Torr xenon-filled lamp having a 4mm bore diameter and 2.125 inch arc length, which uses an external trigger wire for initiation and does not employ simmering.

The simmering of the lamp at a low power level between pulses was first introduced by Yeaman and Creedon as a means of improving lamp life<sup>(2)</sup>; however, it was later found to significantly increase laser output efficiency. (1) A "pseudo-simmer mode" of operation was subsequently developed by ILC in order to reduce the weight of the power supply required.

This technique involves prepulsing the lamp for a period of approx-

imately 100 $\mu$ s before the main pulse is initiated.<sup>(1)</sup> The increase in laser efficiency that resulted from employment of the simmer mode of operation is shown in Table II and Figure 2. The pseudo-simmer mode is being further investigated during this program.

Figure 1 shows the laser output for two lamps operating between 4 and 10 joules energy input. In the case of the 3000 Torr krypton, 3mm bore lamp the laser efficiency is 1.7% at 5 joules and 2.05% at 10 joules, using the full simmer mode of operation. Subsequent laser data obtained at International Laser Systems, Inc. gave a laser efficiency of 2.32% at the 10 joules level, with a 1500 Torr krypton, 3mm bore lamp and external trigger initiation.<sup>(1)</sup> Accordingly it would appear that with full simmer operation approaching 3% efficiency should be realized at the 10 joule lamp energy input level with a 3mm bore 3000 Torr krypton lamp.<sup>(1)</sup>

Further improvements in flash lamp efficiency may be obtained by analyzing the requirements of the driving circuit more closely for the 5 joule and 10 joule modes of flashlamp operation, as it has been found that at these energy levels the plasma does not completely fill the lamp bore. Prior analyses have assumed that the plasma does fill the bore for substantially the whole pulse.<sup>(3)</sup>

The match of the PFN to a flashlamp has been optimized in prior work using a driving circuit analysis due to Markiewicz and Emmett.<sup>(3)</sup> These authors used the relationship

$$v = \pm K_0 \left| i \right|^{1/2} \quad (1)$$

to develop their analysis, where  $v$  is the instantaneous flashlamp voltage corresponding to the instantaneous current  $i$  through the flashlamp.  $K_0$ , the impedance characteristic, is in units of ohm-amps<sup>1/2</sup>. The units of  $K_0$  are derived from the relationship

$$v = R \cdot \left| i \right| \quad (2)$$

where  $R$  is the varying resistance of the flashlamp at a given value of  $v$  and  $i$ .

**TABLE II**  
**IMPROVEMENTS IN LAMP USEFUL LIGHT OUTPUT**  
**AND LASER OUTPUT**

Averaged Values @ 60 Microsecond Lamp Pulse†\*

<u>Modification</u>	<u>Lamp Useful</u>		<u>Laser Output Increase</u>	
	<u>5 Joule†</u>	<u>10 Joule†</u>	<u>5 Joule†</u>	<u>10 Joule†</u>
Xe to Kr	10%	0%**	29%	10%
450 Torr to 3000 Torr	43%	17%	26%	12%
4mm to 3mm	4%	4%	23%	12%
External Trigger to Simmer Mode	63%	25%	62%	30%
Expected Improvement if all effects are independent	168%	52%	225%	81%
Measured Improvement	(Not measured)	56%	240%	72%

\*The comparison is made at this pulse length because this is the pulse length at which the laser data was taken.

\*\*Improvements (of up to 20%) are noted for longer pulse lengths.

†Level of energy level input to lamp.

NOTE: Lamp arc length is 2.125 inches.

Equation 1 is based on earlier experimental work due to Goncz<sup>(4)</sup> who found that for the high current region and with the plasma filling the flashlamp bore the equation

$$v = v_e + |i| \cdot \frac{\gamma l}{A} \quad (3)$$

holds, where  $\gamma$  is the specific resistivity of the xenon or krypton plasma, and is a function of the current density. The voltage drop at the electrodes,  $v_e$ , is of the order of 20V and so can be neglected in comparison with total lamp voltage drop.  $A$  is the cross-sectional area of the tube and  $l$  is its length.

Goncz experimentally found for xenon at 450 Torr that

$$\gamma = 1.13/J^{1/2} \text{ ohm-cm} \quad (4)$$

where  $J$  is the current density, in amps/cm<sup>2</sup>.

From equations 2 and 3:

$$R = \frac{\gamma l}{A} \quad (5)$$

$$v = 1.27 \frac{l}{d} \cdot \frac{1}{i^{1/2}} \quad (6)$$

where  $d$  is the diameter of the flashlamp bore.

Thus

$$v = 1.27 \frac{l}{d} i^{1/2} \quad (7)$$

making

$$K_o = 1.27 \cdot \frac{l}{d} \quad (8)$$

The value of 1.27 holds for 450 Torr Xe lamps. It has been found from many flash lamp experiments run at ILC that equation (8) can be generalized for other pressures and expressed as

$$K_o = k \left( \frac{P}{450} \right)^{0.2} \cdot \frac{l}{d} \quad (9)$$

where P is the flash lamp pressure in Torr. The value of k changes for different gases, and is 1.27 for xenon. The value obtained for krypton has been found to be slightly lower. (1)

Markiewicz and Emmett(3) begin their flash lamp driving circuit analysis by considering the nonlinear differential equation for a single mesh flashlamp LC driving circuit with a voltage  $V_o$  across the capacitor. The nonlinear equation relating L, C and V is:

$$L \frac{di}{dt} \pm K_o |i|^{1/2} + \frac{1}{C} \int_0^t |i| dt = V_o \quad (10)$$

where t is the time in seconds.

If we make the substitutions and normalizations

$$Z_o = \sqrt{\frac{L}{C}}, \quad |i| = I \frac{V_o}{Z_o}, \quad \tau = \frac{t}{T}, \quad (11)$$

$$T = \sqrt{LC} \quad (12)$$

The equation becomes

$$\frac{dI}{d\tau} \pm (\alpha) |I|^{1/2} + \int_0^\tau |I| d\tau = 1 \quad (13)$$

where

$$\alpha = \frac{K_o}{(V_o Z_o)^{1/2}}$$

The quantity  $\alpha$  is called the damping factor for the circuit. The optimum matching of the flashlamp circuit occurs when  $\alpha = 0.8$ .

Gorcz has speculated that the experimental relationship determined in equation (6) might also hold during the initial portion of the pulse, with the effective instantaneous diameter of the arc replacing the bore diameter during the growth period. Thus equation (6) can be restated as

$$R = 1.27 \frac{L}{d_a} \cdot \frac{1}{i^{1/2}} \quad (14)$$

and

$$K_o = 1.27 \frac{L}{d_a} \quad (15)$$

where  $d_a$  is the instantaneous diameter of the arc. Liberman, et al., furnished some experimental support for this hypothesis by applying a variation of equation (14) to the terminal case of arc growth for 0.75J, 20 $\mu$ s pulses in a 3mm bore xenon flash lamp. "At the peak of the current pulse the arc diameter was calculated to be 1.9mm. It appeared to be  $\approx$  2mm to the eye". (5) They further stated that there did not seem to be enough energy in the pulse to expand the arc to the wall. It should be noted that equation (15) makes  $K_o$  time-dependent. Therefore the Markiewicz-Emmett solutions of equation (11) no longer apply exactly, when the bore is not completely filled.

We might further speculate that the 1/2 power relationship in equation (14) might be replaced by another power relationship during the growth period, and the more general relationship

$$v = K_o \parallel i \parallel^n \quad (16)$$

might apply. Indeed for pulsed non wall-confined alkali metal vapor lamps the value of  $n$  has been found to vary from 0.4 to 0.8 for various lamp fills and pressures, (5) and consequently

$$\alpha = \frac{K_o V_o^{n-1}}{(Z_o)^n} \quad (17)$$

These relationships can be experimentally tested on this program. Equipment has been designed to accurately measure  $v$  and  $i$  and also to record the change of  $d_a$  throughout the pulse.

Data from ILC indicate that 100 to 120  $\mu s$  are required for the diameter of the arc,  $d_a$ , to reach the walls of a 4mm bore lamp. This time is much longer than that assumed by Goncz<sup>(4)</sup> based on earlier work reported by Le Compte and Edgerton.<sup>(7)</sup> Consequently, for the short pulse times of 60-200  $\mu s$  considered for pulsed laser applications, a more thorough analysis and experimental determination of the growth mode of the arc is in order, to assure that lamps are operated in the most efficient manner.

Surprisingly, though, it has been experimentally determined that xenon flash lamps operated with high current, short pulses (for example, as dye laser pumps), follow the Markiewicz and Emmett flash lamp model with good accuracy. The probable explanation can be best obtained by rewriting equation (10) as follows:

$$\left[ L + L_a(t) \right] \frac{di}{dt} \pm K_0 i^{1/2} + i \frac{dL_a(t)}{dt} + \frac{1}{C} \int_0^t i dt = V_0, \quad (18)$$

During the arc expansion process the arc has not yet entirely filled the bore, so  $K_0$  is both higher than calculated and is changing in a fashion similar to that expressed in equation (15). The  $K_0 i^{1/2}$  term is, therefore, higher during the arc expansion process.

On the other hand, the  $i \frac{dL_a(t)}{dt}$  term can have a very large negative value, since the inductance of the arc, initially high because of the small arc diameter, is rapidly changing to a low value as the arc expands. These two effects tend to cancel each other in the high current, short pulse regime.

The use of  $\alpha = 0.8$  (the PFN design criterion) often produces component values of  $L$  and  $C$  that are not readily obtainable, so that a departure from  $\alpha = 0.8$  is often obtained. The  $L$  and  $C$  components can be adjusted experimentally to give a value close to 0.8. The criteria used is that at  $3 \sqrt{LC}$  the normalized current is 20% of maximum and at  $4 \sqrt{LC}$  it is essentially zero. A slightly over-damped pulse ( $\alpha$  greater than 0.9<sup>(3)</sup>) is aimed for rather than an

under-damped pulse as current reversals associated with under-damped pulses tend to shorten electrode, and hence, lamp life. The flash lamp circuit parameters for the most efficient 10J lamp developed to date is given in Table III.

TABLE III  
OPTIMIZED FLASHLAMP-CIRCUIT PARAMETERS  
FOR THE MOST EFFICIENT LAMP DEVELOPED  
ON THE PRIOR PROGRAM

Lamp Number	101	
Bore Diameter	3	mm.
Arc Length	2.12	inches
Gas		Krypton
Pressure	1500	Torr
Inside Wall Area	5.1	Sq. cm.
Cross Section Area	0.07	Sq. cm.
Volume	0.38	cc.
Lamp Impedance	27.1	Ohm (Amp) <sup>0.5</sup>
Input Energy	10	Joules
Pulse Width	70	Microseconds
Pulse Rep. Rate	20	Pulses/sec.
Capacitance	20.4	$\mu$ F
Inductance	26.6	$\mu$ H
Voltage	989	V
Circuit Impedance	1.1	$\Omega$
Peak Current	433.3	A
Peak Current Density	6129	A/cm <sup>2</sup>
RMS Current	11	A
Init. Rate Current Rise	37.1	A/ $\mu$ s
Peak Power	214	kW
Average Power	200.0	W
Peak Power Density	562	kW/cc
Ave. Power Density	524.1	W/cc
1 Shot Explosion Energy	192	Joules
Fraction of Explosion Energy	0.65	
Expected Life	>10 <sup>6</sup>	Pulses
Inside Wall Load	39.3	W/cm <sup>2</sup>
Alpha	0.80	

\*K<sub>0</sub> the lamp impedance is measured in ohms-amps<sup>1/2</sup>.

#### 4.0 IMPROVING LASER OPERATING EFFICIENCY

Work was carried out during this reporting period toward development of a 10J lamp that will pump a Nd:YAG laser with 4% overall efficiency. A baseline lamp against which improvements have been measured is the 10J, 4mm bore, 2.125 inch arc length, 450 Torr xenon lamp, which is the standard lamp used in many laser systems including target designator systems. This lamp was also the base comparison lamp used in a prior optical pump program.<sup>(1)</sup> The base line for this program is a modified version of this lamp, which is presently being used in field tests. It is the same lamp filled to 1500 Torr. This modified lamp will soon be used in target designator and illuminator systems. The optimized flashtube, lamp and circuit parameters for the best lamp developed on the prior program are given in Table III. It, too, can be used as a comparison lamp.

Techniques to increase both the amount of effective light output (effective irradiance) and effective brightness (effective radiance) are required, as both quantities contribute to increase the efficiency of laser pumping. The work "effective" is used to denote that portion of the light output of the lamp that can be used to pump the excitation bands of the laser. Therefore, differential fluorescence analysis measurements (proportional to effective light output) and arc diagnostic tests are programmed. Laser testing will provide confirmation of the improvements obtained.

#### 4.1 Lamps with Cerium Doped Quartz Envelopes

Quartz doped with cerium will absorb radiation below  $0.31 \mu\text{m}$  and will fluoresce at wavelengths between  $0.4$  and  $0.65 \mu\text{m}$ . A sample of 4mm bore diameter cerium doped quartz became available and a lamp with a 2.0 inch arc length was constructed from it. A control lamp was constructed from clear fused quartz envelope material with the same dimensions. Both lamps were filled with 450 Torr of xenon.

Spectral data was taken on both lamps at 10 joules input energy and are shown in Figure 3. The cerium doped envelope lamp has approximately 15% greater output over the spectral range from  $0.4$  to  $0.65 \mu\text{m}$ . Since Nd:YAG has a pump band in the wavelength region from  $0.57$  to  $0.60 \mu\text{m}$  (Figure 4) the increased output in the  $0.57$  to  $0.60 \mu\text{m}$  region should increase the pumping efficiency.

Laser tests will be conducted later to measure the efficiency improvement that can be obtained when using cerium doped quartz as an envelope material.

#### 4.2 Operation of Lamps in Simmer Mode

Prior investigation(1) has shown that operation of lamps with a "simmer current" or "keep alive current" increases both the total light output and the useful light output from lamps. Comparative data of useful light output for simmer and external trigger modes of operation are shown in Figure 5 for a 450 Torr xenon filled lamp with 4mm bore diameter. Comparative laser data for the same lamp operated alternatively with external triggering and with simmer mode are shown in Figure 2. The useful light output at 10J input energy is increased approximately 29%, and the laser output is increased by 27%.

A theoretical investigation was undertaken to determine the reason for the increased efficiency of light production. As a part of this investigation an energy level diagram for krypton was constructed and is presented in Figure 6. The main lines that contribute to pumping of a Nd:YAG laser are indicated, and are seen to terminate on the metastable level.

A spectrum from a krypton lamp is shown in Figure 7, before and after going through a Nd:YAG filter. It is seen that the lines that pump Nd:YAG most effectively are at 0.7602, 0.8104 and 0.8113 $\mu$ . (The latter two lines are not resolved in the spectra.) On the energy level diagram these lines terminate at the metastable level at 7.98 eV.

Simmer current can affect the light output of the main discharge by providing the presence, at the beginning of the pulse, of ions and electrons of the simmer discharge, and the resulting metastable and resonance-excited atoms. The metastable atoms in the gas outside the simmer discharge column increase the rate of growth of the arc when the main discharge is initiated. The arc grows by means of heat conduction to the gas at its boundary, and also by electron-impact ionization of neutral atoms in the boundary layer. If metastables are present, this ionization proceeds at a faster rate, and the boundary layer becomes ionized at a lower temperature than is the case when there are no metastables initially present. The result is that, in the simmer mode,

the arc is larger and has a lower impedance at any given value of current during its growth, than is the case for non-simmer operation. Since the voltage gradient is lower during arc growth in simmer operation, the electron temperature is also lower. And while the peak current is higher (because of the lower voltage gradient) the current density is lower (because of the larger arc diameter). The lower current density and the lower electron temperature both reduce the relative importance of continuum radiation as compared to line radiation. Since the line radiation is in the Nd:YAG pumping band, the effect of simmer mode operation is to increase the fraction of the output energy that is within the Nd:YAG pumping band.

In addition, the image of the larger arc can fill the laser rod more uniformly, probably giving a higher laser efficiency.

#### 4.3 Triggering Improvements

The usual wrapped trigger wire produces an initially spiral or stepped arc in flash lamps; the plasma follows the placement of the trigger wire along and around the lamp. It was reasoned<sup>(1)</sup> that if the plasma could be maintained in a straight line during the arc growth phase, then the imaging of the radiation from the lamp onto the laser rod would be improved. The effective brightness should also increase. Both of these effects should lead to an improved efficiency of laser output.

A straight trigger conductor was made by plating a thin strip of nickel-layered-over-silver on the side of the flash lamp. Previous attempts to accomplish this involved painting the strip onto the lamp but were unsatisfactory, with the strips disintegrating after a brief pulsing period. This time a durable strip was deposited onto the lamp by using a recently developed technique, called "ion plating".

In order to measure the improvements in arc control obtained by this technique, a diagnostic tool was required that could measure and record arc growth and position as a function of time. Accordingly, a device has been developed that is capable of photographing the arc growth for any  $2\mu$ s interval during the flash lamp light pulse. The block diagram of the device is shown in Figure 8. An image

intensifier tube is energized for  $2\mu s$ , and performs the function of an extremely high speed shutter. A delay line controls the time when the shutter opens, thereby making it possible to photograph the arc during any portion of its growth and decay. A camera lens focuses the arc image on the image intensifier tube target. A Polaroid oscilloscope camera photographs the arc image on the tube screen. Filters of the appropriate density are inserted in the optical path to adjust the light intensity to fall within the proper exposure range of the film. Figure 9 is a photograph of the equipment.

The pulse command triggers the lamp circuit and a delay line. Experience has shown that successive arc discharges in any lamp (over the relatively small number of pulses used in these tests) are similar in appearance, so that a growth sequence may be photographed by exposing for one successive segment per flash for a number of pulses.

An L349 lamp (4mm bore, 2.125 inch length, with Xe gas at 450 Torr) was modified by adding a plated strip trigger wire. This lamp is designated the L349A. It was photographed with pulse input energies of 5 through 60 joules. The percentage of the lamp bore filled at the peak of the current pulse as a function of input energy is shown in the series of photographs presented in Figure 10 and graphically summarized in Figure 11. With energy inputs of less than 20 joules the arc does not fill the bore.

The growth of the arc of 5 and 10 joule pulses with both types of trigger wire is clearly portrayed in the time sequence of arc photographs presented in Figures 12 through 15. The helix effect observed when using the normal trigger wire is clearly seen in the photographs, in contradistinction to the smooth radial growth of the arc in the striped lamp. Further details of the smooth arc growth of the L349A in the vicinity of the cathode are presented in Figure 16. These data are presented in another form in Figures 17 through 20, again demonstrating the more regular growth of the arc in the L349A lamp, especially at the 5 joule level.

It is expected that the control of plasma arc growth achieved with the L349A lamp will result in improved laser output because of increased brightness of the arc and improved imaging of the arc on the laser rod. Laser tests are scheduled on both the L349 and L349A lamps.

## 5.0 IMPROVING LASER OPERATING REPRODUCIBILITY

A goal of the program is to achieve reproducibility of laser light output within  $\pm 5\%$ , from pulse to pulse and from lamp to lamp. The figure must be translated into terms of lamp light output reproducibility. Optimized lamp and power supply parameters are shown in Table IV and Table V for the two modes of operation given in Table I. It will be assumed initially that variations in lamp light output will have a linear relationship with variations in laser output when using a given laser system in which everything, including the PFN, is held constant except the lamp itself. (The exact relationship will be determined in this program.)

It is worth noting at this point that the reproducibility of light output for a given energy input can be accurately determined separately from the absolute output value. The reproducibility can be measured by repeating the tests and calculating the deviations of the multiple tests. The absolute output value can only be determined by comparing the light output or energy input with calibrated standards traceable to NBS. For the purposes of this program we are concerned primarily with reproducibility.

One reasonable way to restate the requirement that the reproducibility of laser output shall initially be within  $\pm 5\%$  is to assume normally distributed variations in light output and to require that a large number of the lamps must have 99.7% ( $3\sigma$  limits) of their laser test results within a  $\pm 5\%$  range.

Table VI shows that for a sample size of 21 normally distributed units all of those units must have test results within a range of  $\pm 1.5\%$  to have 90% confidence that 99.7% of a large population will have test results within a range of 5%.

### 5.1 Analysis of Lamp Variables

The primary variables in the lamp construction that can influence the lamp light output are fill pressure, bore diameter, and arc length. Lamp processing can also affect light output. For example, cathode deposits on the tube walls cause a reduction in light output with usage. Parametric analysis of these variables shows that light output variations are only weak functions of fill pressure and arc length, but are a strong function of the arc diameter. The arc diameter in turn is a complex function of the instantaneous current, the interval since pulse initiation,

and bore diameter. Additional analysis is planned in order to obtain detailed insights into bore diameter effects on light output reproducibility. It may be noted already, however, that the effect of bore diameter on light output appears to operate through the effect of arc diameter on  $\alpha$ , the damping coefficient; non-optimal values of  $\alpha$  result in slower energy delivery to the lamp and, consequently, less output per unit time.

TABLE IV  
MODE I OPERATION  
OPTIMIZED FLASHLAMP-CIRCUIT PARAMETERS

Lamp Number	102	
Bore Diameter	3	mm
Arc Length	1.00	Inches
Gas		Krypton
Pressure	1500	Torr
Inside Wall Area	2.4	cm <sup>2</sup>
Cross Section Area	0.07	cm <sup>2</sup>
Volume	0.18	cc.
Lamp Impedance	12.8	Ohm (Amp) <sup>0.5</sup>
Input Energy	5	Joules
Pulse Width	70	$\mu$ s
Pulse Rep. Rate	1	Pulses/Sec.
Capacitance	44.3	$\mu$ F
Inductance	12.3	$\mu$ H
Voltage	475	V
Circuit Impedance	0.5	$\Omega$
Peak Current	451.0	A
Peak Current Density	6379	A/cm <sup>2</sup>
RMS Current	1.2	A
Init. Rate Current Rise	38.7	A/ $\mu$ s
Peak Power	107	kW
Average Power	5	W
Peak Power Density	497	kW/cc
Ave. Power Density	27.8	W/cc
1 Shot Explosion Energy	91	Joules
Fraction of Explosion Energy	0.66	
Expected Life	>10 <sup>6</sup>	Pulses
Inside Wall Loading	10.4	W/cm <sup>2</sup>
Alpha	0.80	

TABLE V  
MODE II OPERATION

OPTIMIZED FLASHLAMP-CIRCUIT PARAMETERS

Lamp Number	103	
Bore Diameter	4	mm
Arc Length	2.12	inches
Gas		Xenon
Pressure	1500	Torr
Inside Wall Area	6.8	cm <sup>2</sup>
Cross Section Area	0.13	cm <sup>2</sup>
Volume	0.68	cc
Lamp Impedance	22.8	Ohm (Amp) <sup>0.5</sup>
Input Energy	10	Joules
Pulse Width	70	μs
Pulse Rep. Rate	20	Pulses/Sec.
Capacitance	25.7	μF
Inductance	21.2	μH
Voltage	882	V
Circuit Impedance	0.9	Ω
Peak Current	485.6	A
Peak Current Density	3864	A/cm <sup>2</sup>
RMS Current	13	A
Init. Rate Current Rise	41.6	A/μs
Peak Power	214	kW
Average Power	200.0	W
Peak Power Density	316	kW/cc
Ave. Power Density	294.8	W/cc
1 Shot Explosion Energy	257	Joules
Fraction of Explosion Energy	0.04	
Expected Life	>10 <sup>6</sup>	Pulses
Inside Wall Load	29.5	W/cm <sup>2</sup>
Alpha	0.80	

TABLE VI  
OBSERVED VARIATIONS REQUIRED TO ASSURE THAT  
99.7% OF POPULATION LIES WITHIN ±5%  
(With 90% Confidence)

<u>Sample Size</u>	<u>Maximum Variation in Sample Values</u>
4	0.5%
7	1.0%
21	1.5%

Notes:

1. Assuming Normal Distribution and Mean at 0% Variation
2. Sample Size for 90% Confidence  
That + 3 Standard Deviations of a large sample  
Lies within ± 5% tolerance

5.2 Fluorescence Analysis Instrumentation

A digital readout system was devised to work with the fluorescence analysis instrument. The readings taken with this equipment are apparently reproducible to ±0.1%, which is appreciably better than readings taken from oscilloscope photographs, ±3%. A schematic diagram of the equipment is shown in Figure 21 and a photograph of the equipment appears in Figure 22. The outputs from the two sensor diodes shown are amplified. The smaller signal is subtracted from the larger signal, and a peak difference signal is produced. The peak difference signal is fed to a sample and hold circuit, and finally the signal is displayed on a digital panel voltmeter. The input energy to the PFN, which is discharged into the lamp, is set by the voltage applied to the capacitor. This voltage is controlled and is measured to an accuracy of ±0.1%.

Table VII shows a series of 10 readings taken on a single

lamp. The average deviation on this lamp, i.e.  $\Sigma \frac{(\text{reading}-\text{mean})}{n}$  is 0.7%.

TABLE VII  
REPLICATE FOV DATA FOR A SINGLE LAMP

<u>Pulse #</u>	<u>Output (mv)</u>	<u>Deviation (mv)</u>
1	1404	20
2	1420	4
3	1444	20
4	1412	12
5	1433	9
6	1413	11
7	1437	13
8	1421	3
9	1433	9
10	1423	1
	<u>14240</u>	<u>102</u>
	<u>14240</u>	<u>102</u>
Average	1424.0	
Average Dev.		10.2
Average Dev. %		0.7%
Max. Dev.		$\pm 1.4\%$

The variations in the FOV readings can be due to variations in both the lamp and the measurement equipment. Lamp and lamp-related effects include:

- a) Variability of PFN energy delivery
- b) Trigger wire placement and arc growth variations

- c) Lamp warm-up
- d) Random fluctuations due to cathode emission
- e) Other, miscellaneous, effects

Measurement equipment variations can be due to:

- a) Changes in the reflectivity of the integrating cavity.
- b) Aging of the Nd:YAG crystal and detectors.
- c) Other factors including circuit noise and differences in diode temperature effects.

Attempts will be made to separate these effects.

### 5.3 Lamp Fabrication

Three experimental approaches were taken to reducing lamp bore diameter variations from the  $\pm 12\%$  characteristic of standard 4mm bore quartz tubing:

- a) 4mm  $\pm 1\%$  tubing was selected from standard 4mm tubing. (Size distributions were taken for several sizes and types and are shown in Figures 23 and 24.)
- b) Precision ground tubing, 4mm bore  $\pm 0.05\text{mm}$ , was ordered.
- c) Oversize tubing was shrunk down over precision ground tungsten rods, which were ground and polished to 4mm  $\pm 0.01\text{mm}$ .

Selecting tubing to the tolerances required appears to be impractical as a manufacturing step from a cost and time viewpoint. Quotations for tubing of 4mm  $\pm 0.05\text{mm}$  tubing tolerances were solicited from seven fabricators of standard quartz tubing, but all "no quoted".

The cost of precision ground tubing, \$15 for a 12 inch section, is high, but not prohibitive for use in production runs of lamps.

The tubing made by shrinking down larger tubing onto the polished tungsten rods was all within  $\pm 0.02$ mm of the size desired. This method is the most suitable, precise, and economical of the methods discussed.

While the alternatives above were being investigated, twenty-eight lamps were constructed with selected tubing of 4mm  $\pm 0.05$ mm bore diameter, and filled with xenon at 1500 Torr. They are scheduled to be life tested after initial measurements of useful light output are performed on them. Lamp deterioration data will be taken as the lamps are life tested.

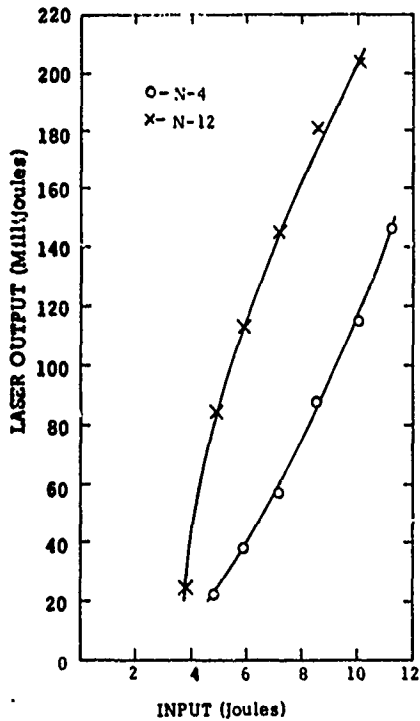
#### 5.4 Life Test Instrumentation

The equipment to life test 5 lamps simultaneously has been completed and evaluated as satisfactory.

The flashlamp life test unit consists of three separate single mesh pulse forming networks to correspond to the three originally specified modes of operation. The capacitance and inductance of the networks can be varied in integral increments. The PFN charge voltage can be varied from 0 to 1500 volts. Each PFN has its associated lamp triggering and failure sensing mechanism. Lamp triggering is accomplished with a series trigger transformer with 18 $\mu$ H saturated inductance driven by a pulse generator. Lamp failure is sensed indirectly by counting lamp fires. The lamp fire signals are integrated and applied to an AND gate, which causes the entire system to shut off in case there is the absence of a fire signal from any of the lamps for 10 consecutive shots.

6.0 REFERENCES

1. L. Noble, J. Moffat, L. Reed and J. Richter, "Optical Pumps for Lasers", Final Report, May 1971 ECOM-0035-F.
2. N. L. Yeamans and J. E. Creedon, "Long-Life High-Repetition-Rate Flash Tubes", R&D Technical Rpt., ECOM-3043, Nov. 1968.
3. J. P. Markiewicz and J. L. Emmett, "Design of Flashlamp Driving Circuits", IEEE J. of Quant. Electr., Vol. QE-2, No. 11, Nov. 1966.
4. J. H. Goncz, "Resistivity of Xenon Plasma", J. Applied Phys., 36, 742 (1965).
5. I. Liberman, et al "Optical Pumps for Lasers - Phase II", Final Rpt. Contr. DA-28-043-AMC-02097 (E), October 1968.
6. L. Noble, "Optical Pumps for Erbium Lasers", Final Rpt., Contr. DAAB07-70-C-0296, October 1971.
7. G. W. LeCompte and H. E. Edgerton, J. Applied Phys., 27, 1427 (1956).



**LASER DATA**

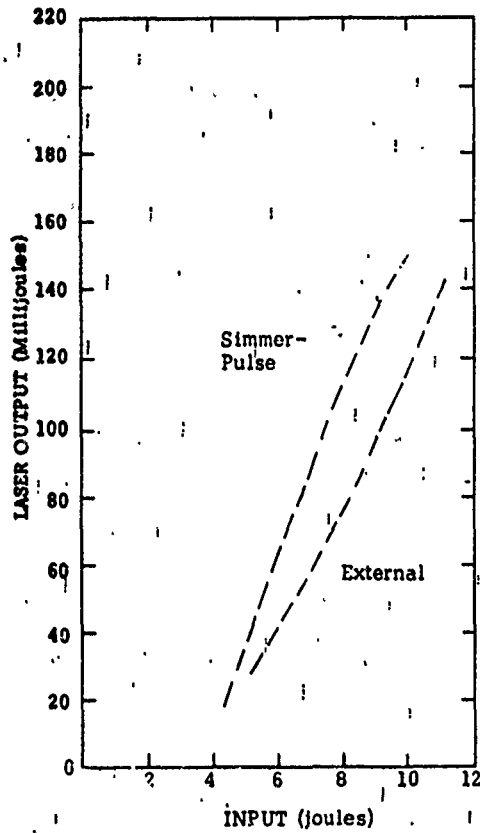
Rod: Nd:YAG, 1/4" x 2-1/2"  
 A/R Coating: None  
 Output Mirror: 55 % Reflective  
 Cavity: Elliptical, Close Wrapped  
 Coolant: Water  
 Inductance: 9 Microhenries  
 Capacitance: 47.3 Microfarads (not critically damped, not optimized)  
 Operating Mode: Normal  
 Pulse Repetition Rate: 10 pps.

**LAMP DATA**

	Lamp N-4	Lamp N-12
Lamp Bore Diameter (mm):	4	3
Lamp Arc Length (inches):	2.125	2.125
Lamp Fill Gas:	Xenon	Krypton
Lamp Fill Pressure (Torr):	450	3000
Initiation Method:	External	Simmer Pulse

FIGURE 1 LASER OUTPUT DATA FOR 3000 TORR KRYPTON LAMP AND 450 TORR XENON LAMP

1034



**LASER DATA**

Rod: Nd:YAG, 1/4" x 2-1/2"  
 A/R Coating: None  
 Output Mirror: 55% Reflective  
 Cavity: Elliptical, Close Wrapped Water  
 Inductance: 9 Microhenries  
 Capacitance: 47.3 Microfarads (not critically damped, not optimized)

**LAMP DATA**

Lamp Bore Diameter: 4 mm  
 Lamp Arc Length: 2.125 inches  
 Lamp Fill: Xenon Gas  
 Lamp Fill Pressure: 450 Torr  
 Initiation Method: Simmer Pulse and External

**FIGURE 2 LASER OUTPUT DATA FOR XENON LAMP FOR SIMMER PULSE AND EXTERNAL TRIGGER OPERATION**

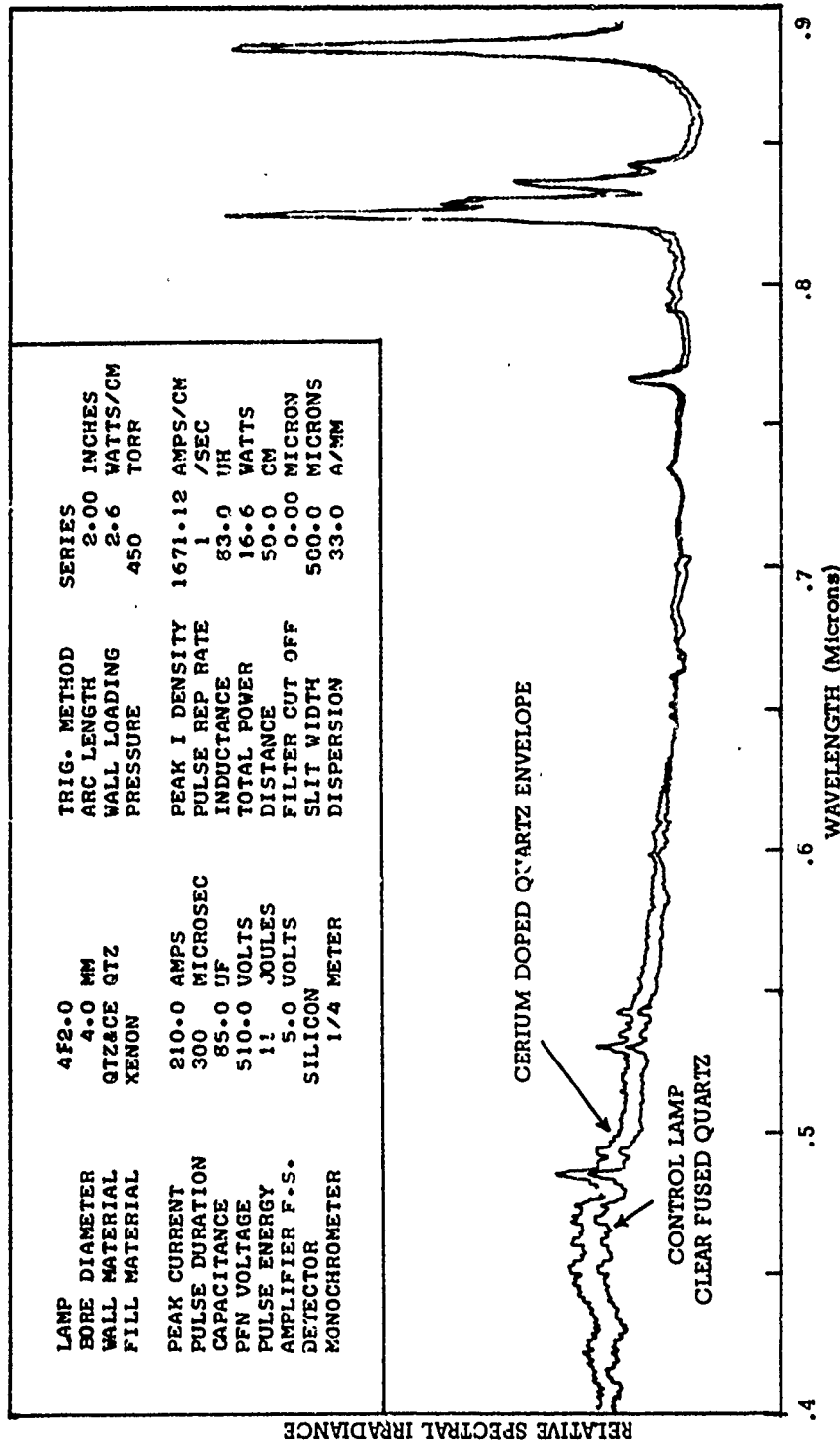


FIGURE 3 COMPARATIVE SPECTRAL DATA FOR A CERIUM DOPED QUARTZ ENVELOPE LAMP AND A STANDARD QUARTZ ENVELOPE LAMP

2902

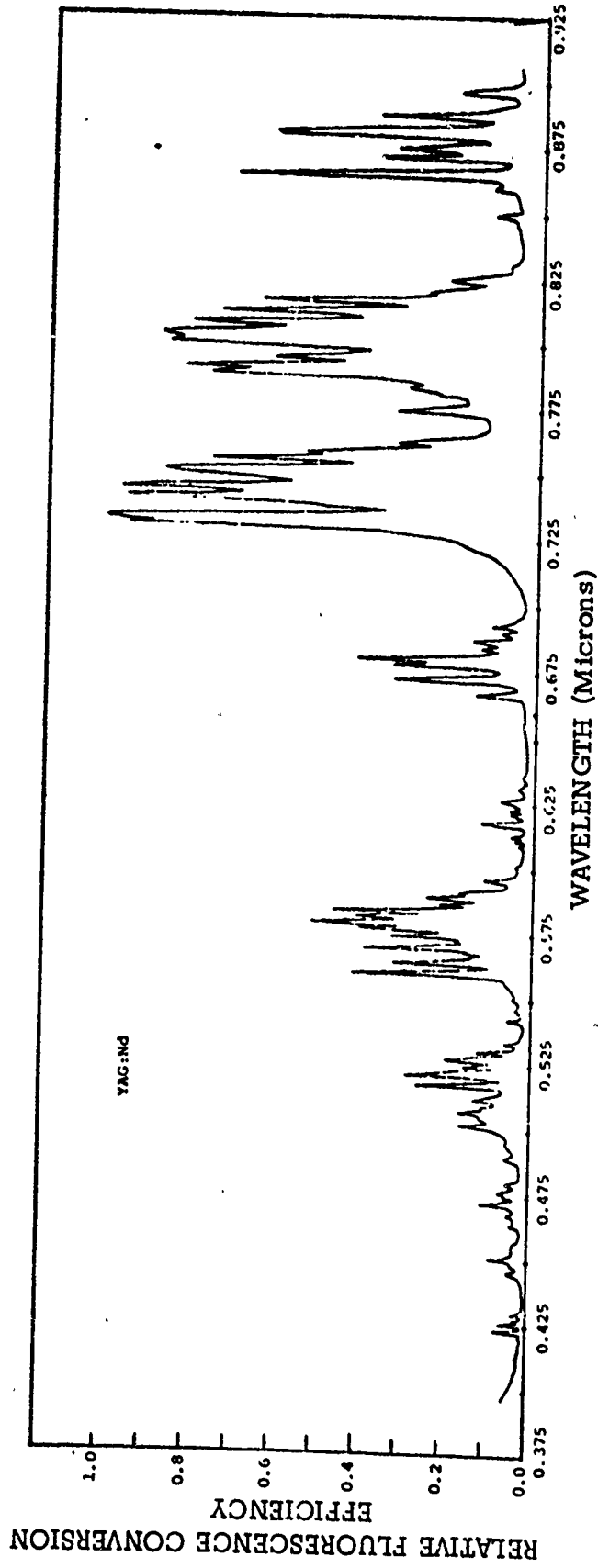
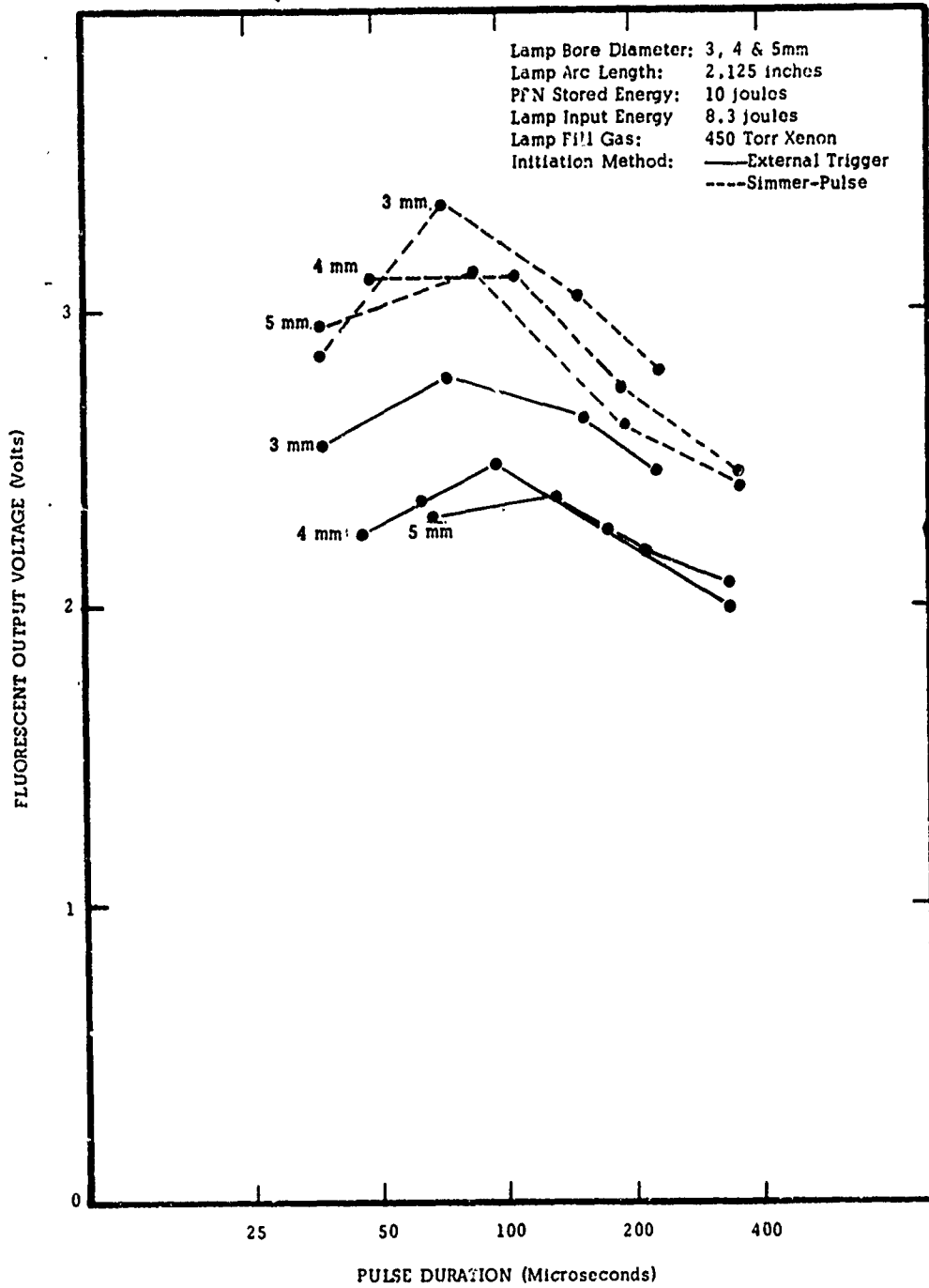


FIGURE 4 EXCITATION SPECTRA FOR Nd:YAG



1018

FIGURE 5 FOV DATA FOR 450 TORR XENON LAMPS, EXTERNAL TRIGGER AND SIMMER PULSE (10 JOULES)

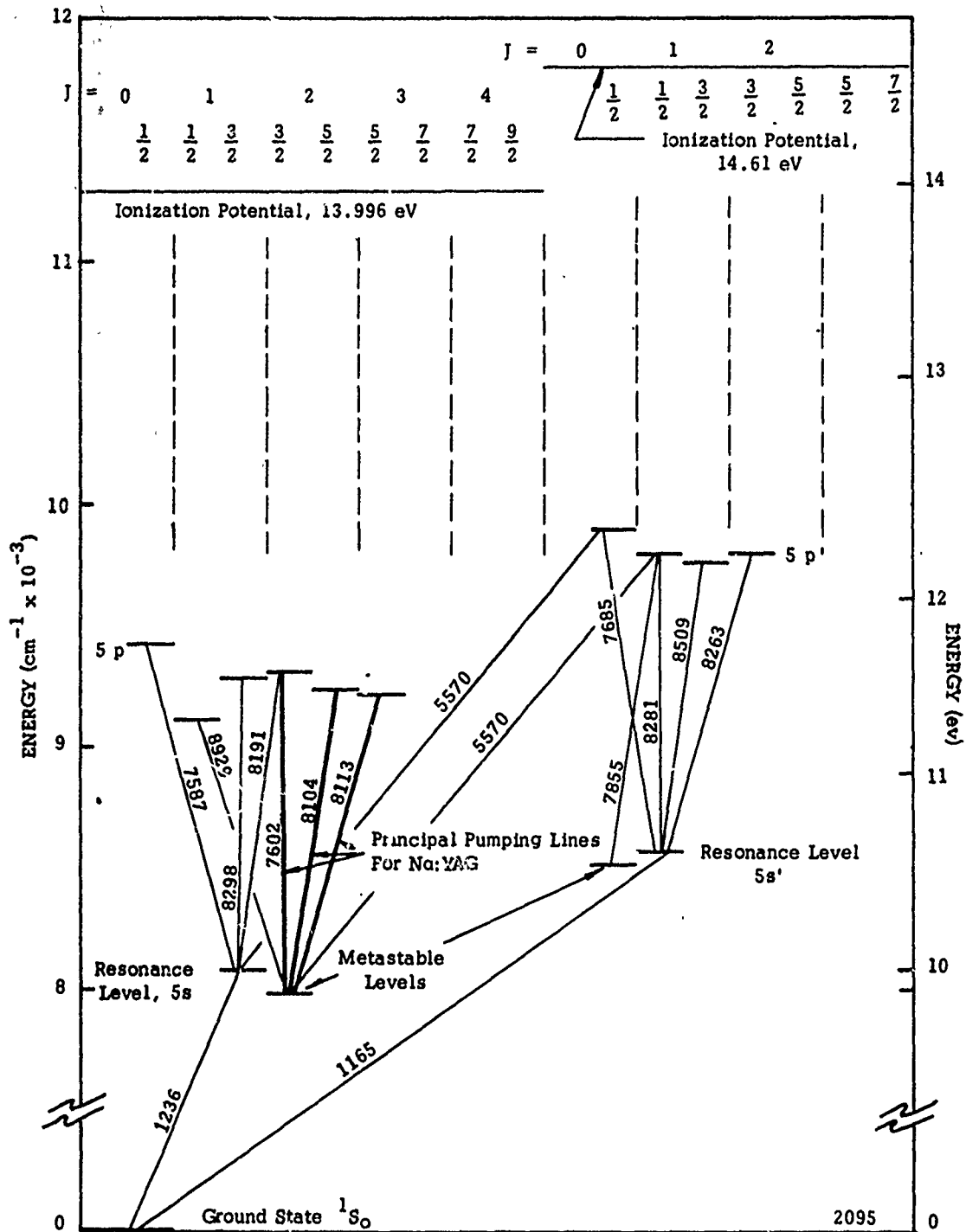


FIGURE 6 GROTRIAN ENERGY LEVEL DIAGRAM FOR KRYPTON

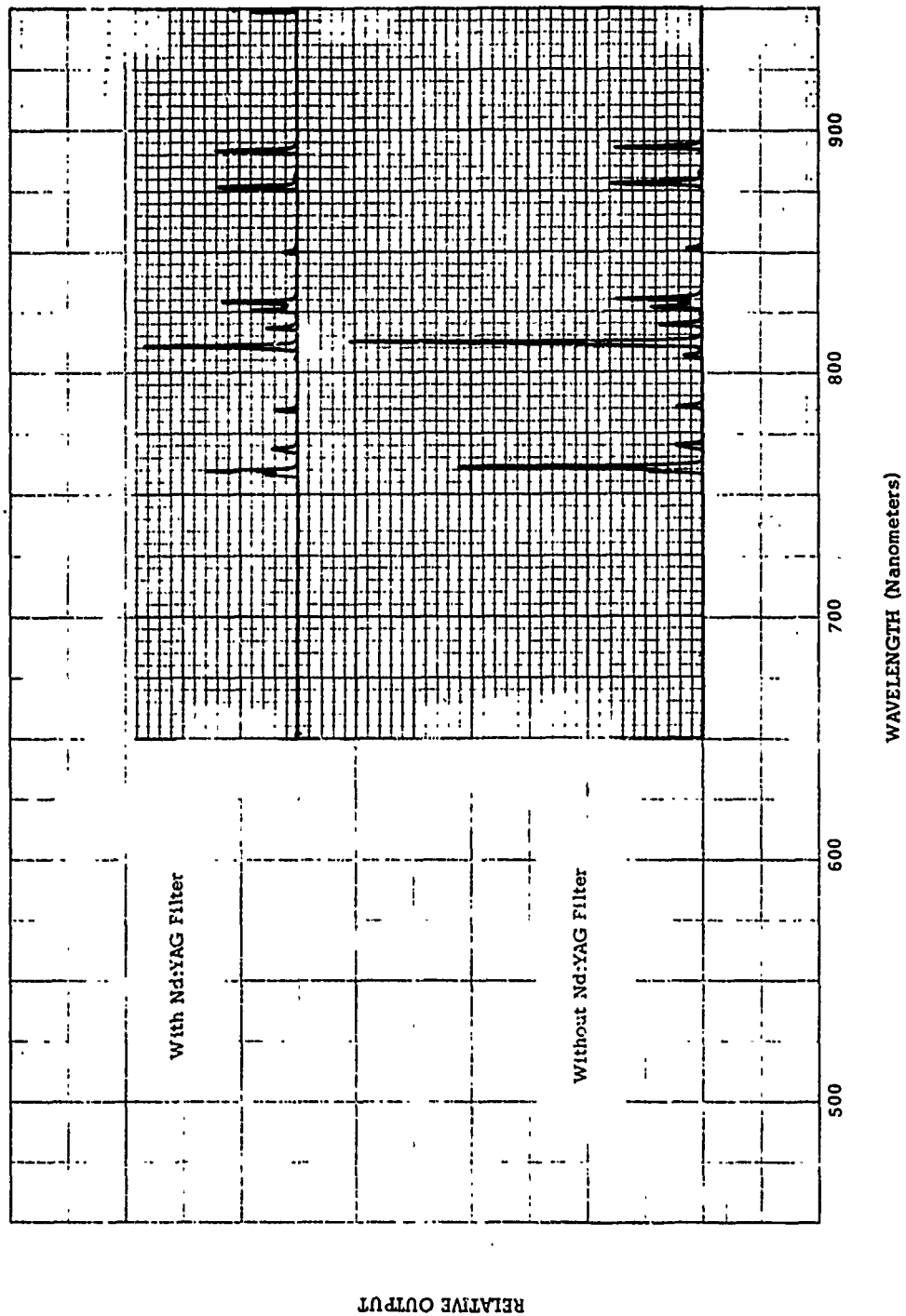


FIGURE 7 EMISSION SPECTRUM AND NON ABSORBED RADIATION OF 4 ATMOSPHERIC KRYPTON LAMP

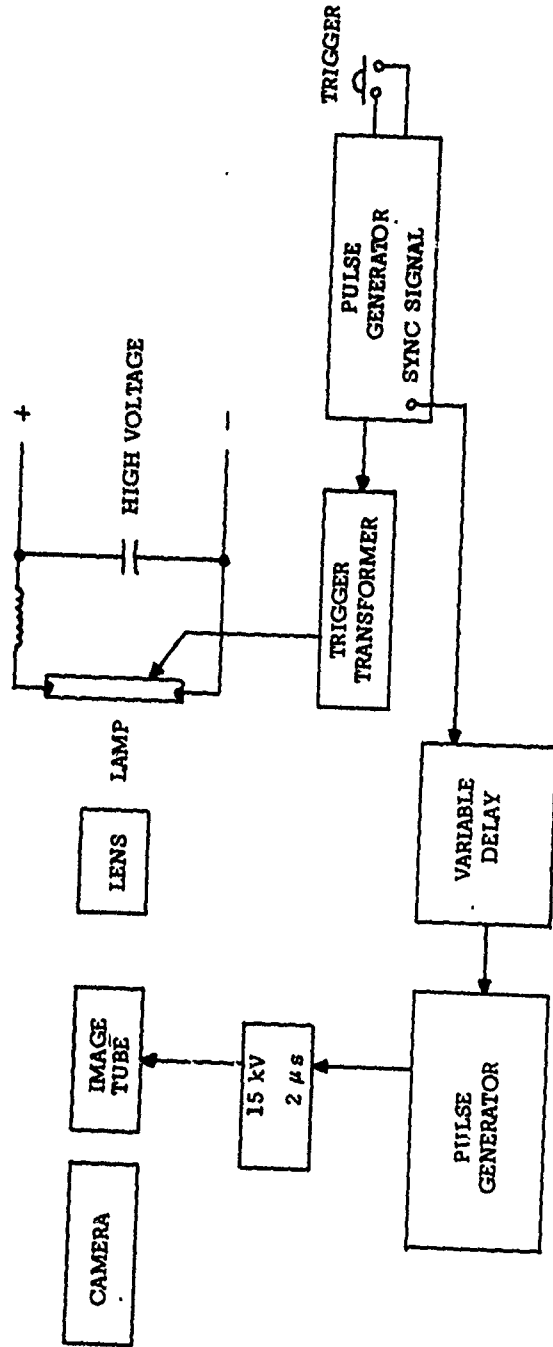


FIGURE 8 BLOCK DIAGRAM OF PULSE ARC GROWTH IMAGE RECORDER

3000

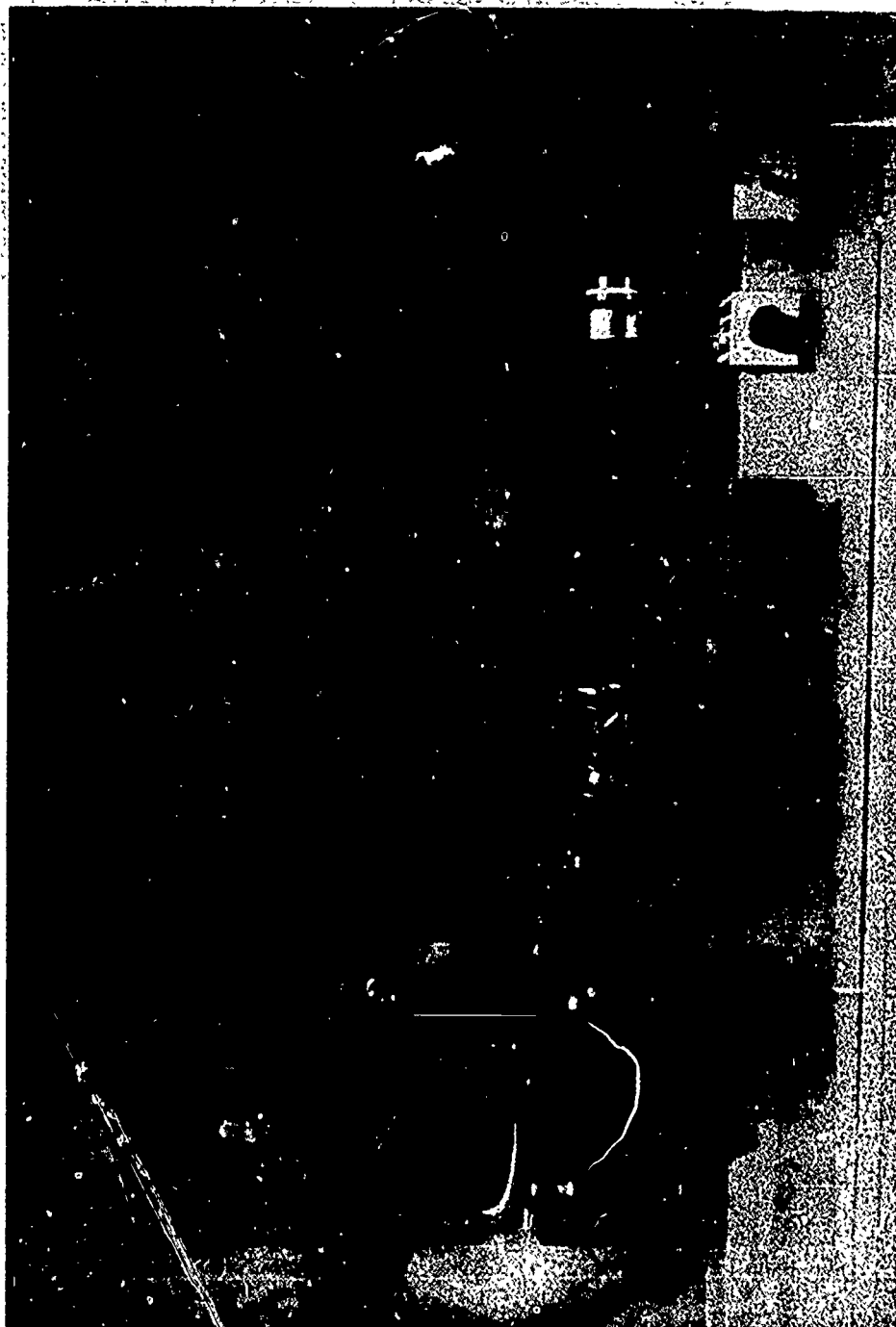
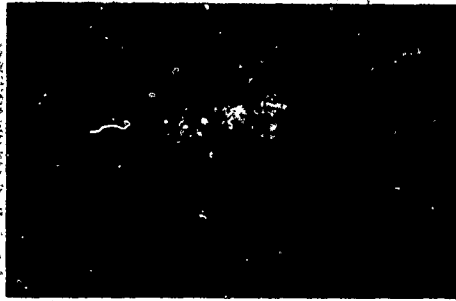


FIGURE 9 PULSE ARC GROWTH IMAGE RECORDER

3001

LAMP L349

5 Joules



Y = 100 Amperes/cm  
X = 20  $\mu$ s/cm

PHOTOGRAPH OF ARC



POSITION OF TUBE WALL

TRIGGER



(SAME SCALE AS PHOTOGRAPH)

10 Joules



Y = 100 Amperes/cm  
X = 20  $\mu$ s/cm



20 Joules



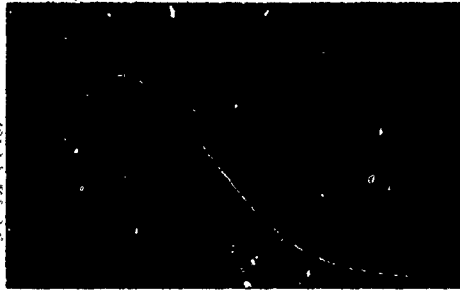
Y = 100 Amperes/cm  
X = 20  $\mu$ s/cm



4003

FIGURE 10A CURRENT-TIME CURVES AND PHOTOGRAPHS OF PLASMA FOR PULSE ENERGIES OF 5, 10, 20, 40 and 60 JOULES

40 Joules

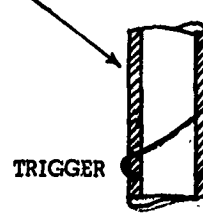


Y = 200 Amperes/cm  
X = 20  $\mu$ s/cm

PHOTOGRAPH OF ARC



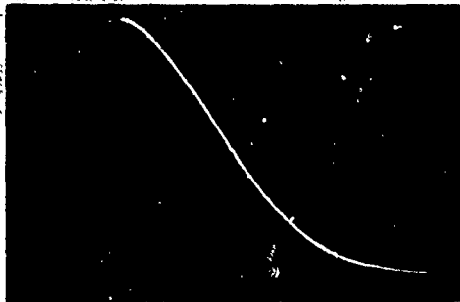
POSITION OF TUBE WALL



TRIGGER

(SAME SCALE AS PHOTOGRAPH)

60 Joules



Y = 200 Amperes/cm  
X = 20  $\mu$ s/cm



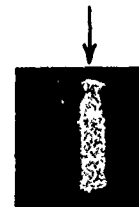
TRIGGER STRIP

Lamp L349A

5 Joules



Y = 200 V/cm -- 100 A/cm  
X = 20  $\mu$ s/cm



4003

FIGURE 10B CURRENT-TIME CURVES AND PHOTOGRAPHS OF PLASMA FOR PULSE ENERGIES OF 5, 10, 20, 40 and 60 JOULES

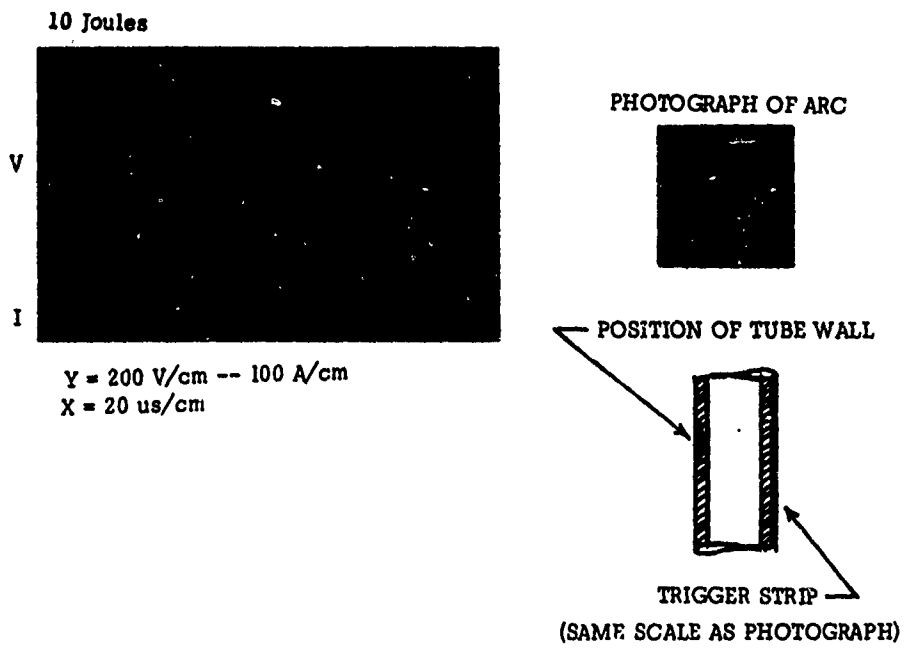


FIGURE 10C CURRENT-TIME CURVES AND PHOTOGRAPHS OF PLASMA FOR PULSE ENERGIES OF 5, 10, 20, 40 and 60 JOULES

MEASURED VALUES  
 INTERPOLATED VALUES  
 L349 SPIRAL WRAP TRIGGER  
 L349A TURBULENT DISCHARGE  
 L349A PLATED STRIPE  
 LAMINAR DISCHARGE

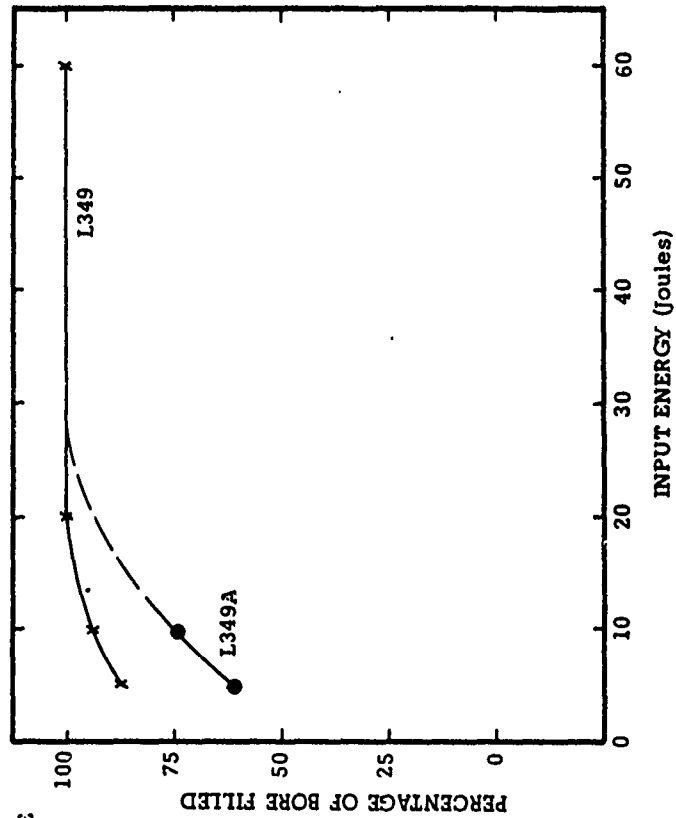


FIGURE 11 PLASMA DIAMETER AS A FUNCTION OF INPUT ENERGY

1000

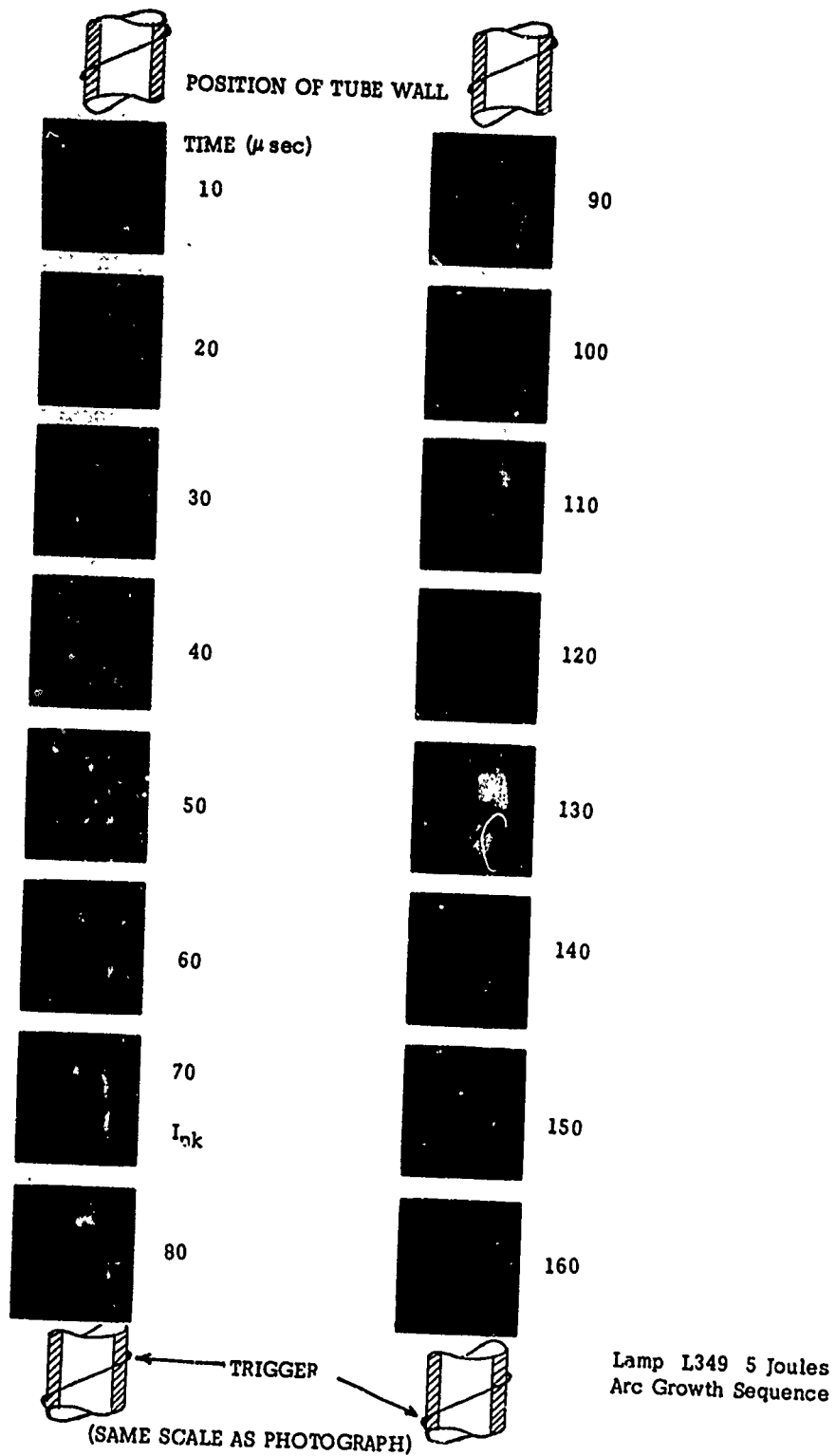
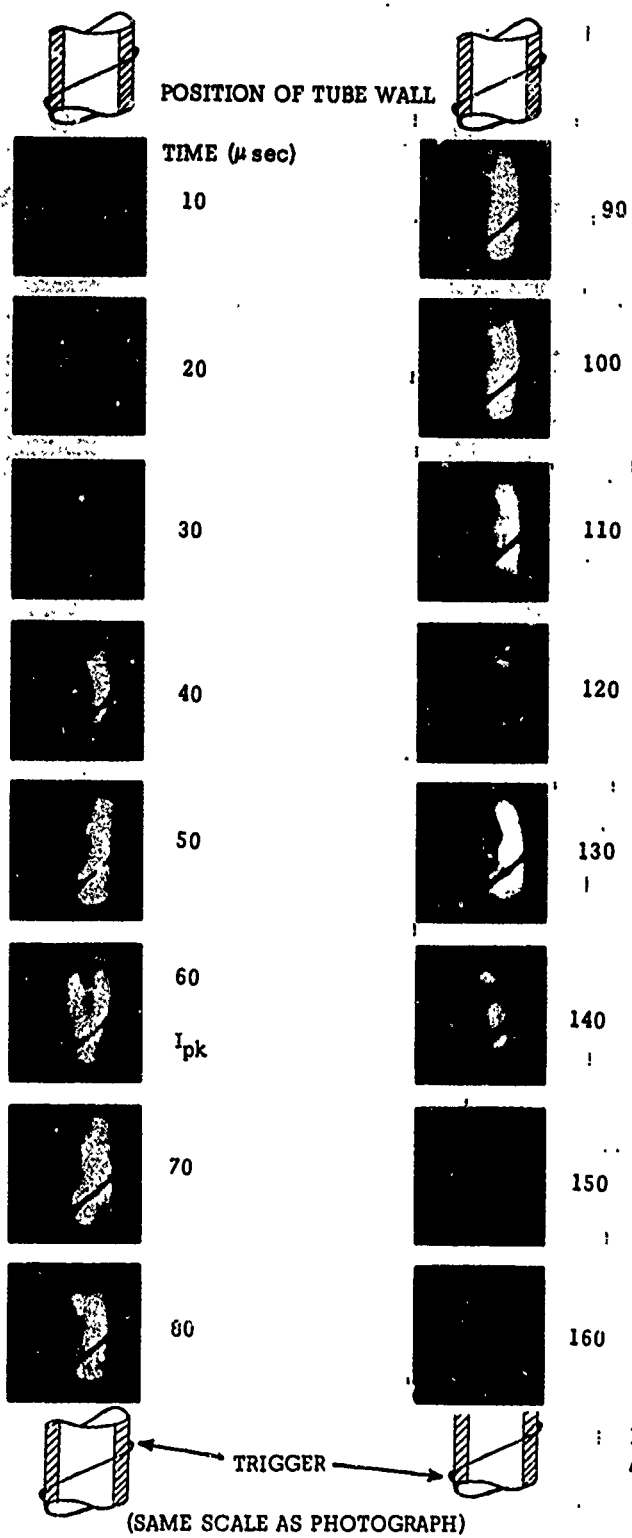


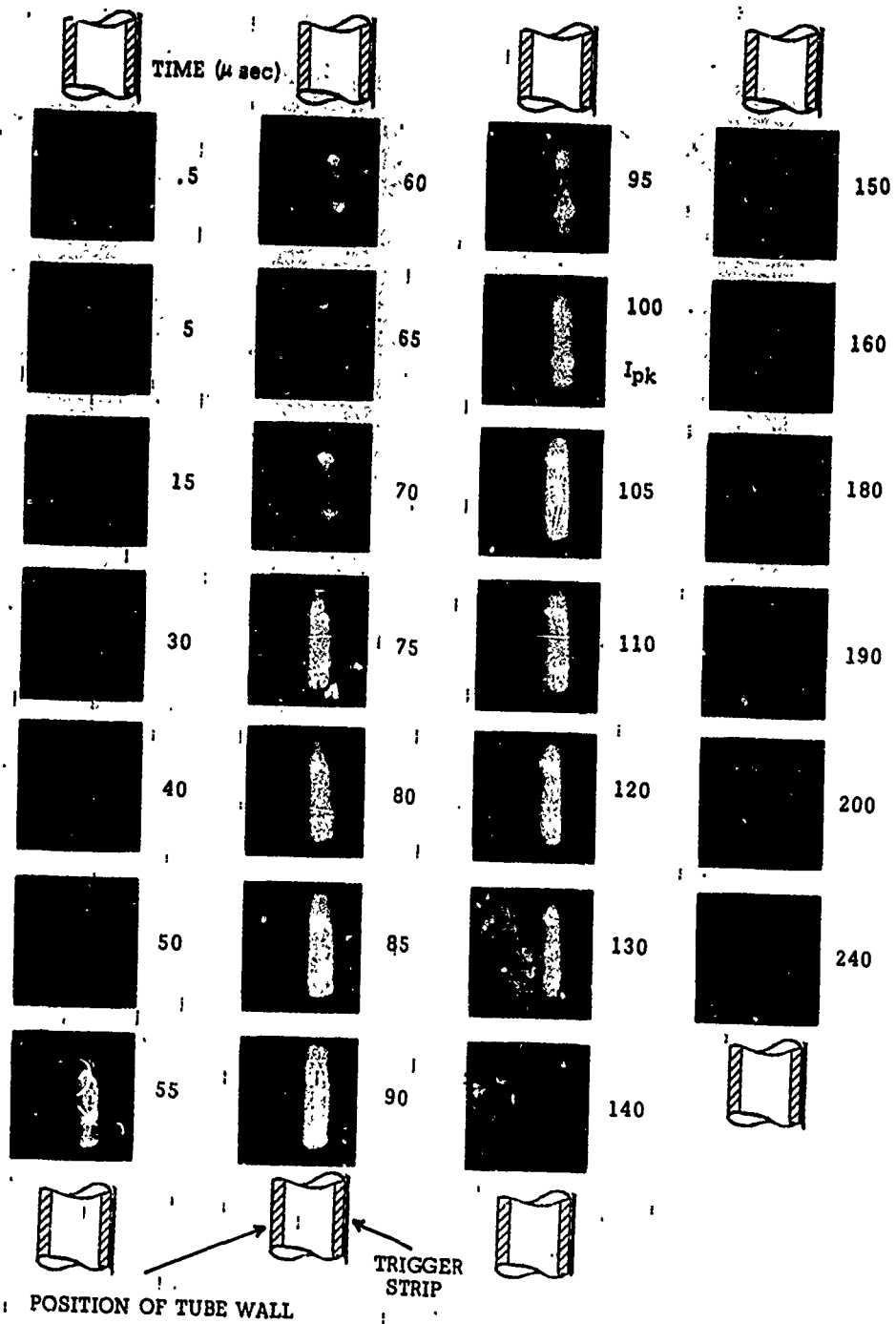
FIGURE 12 PLASMA GROWTH IN L349 AT 5 JOULES



Lamp L349 10 Joules  
Arc Growth Sequence

4002

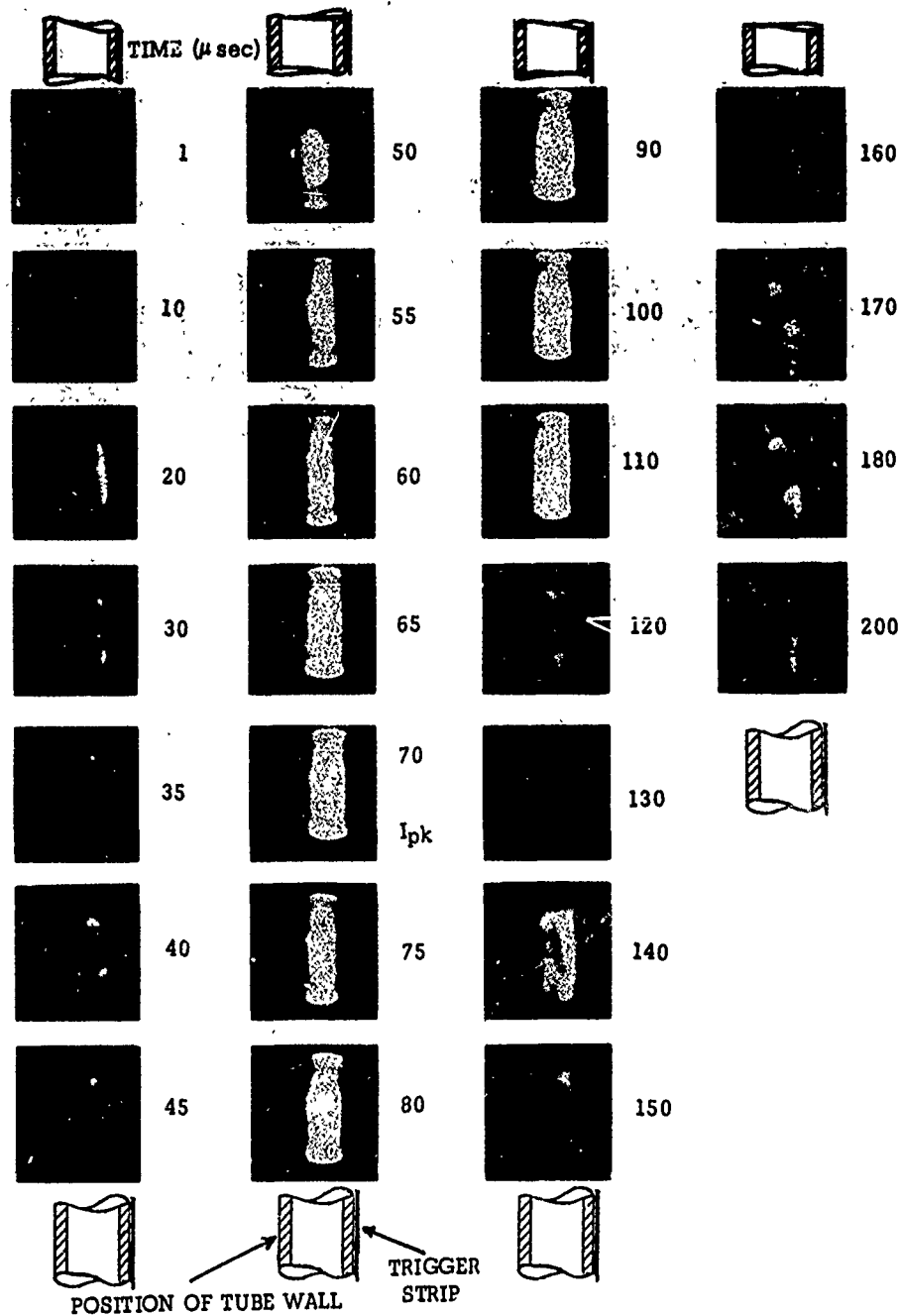
FIGURE 13 PLASMA GROWTH IN L349 AT 10 JOULES



(SAME SCALE AS PHOTOGRAPH)

Lamp L349A 5 Joules  
Arc Growth Sequence

FIGURE 14 PLASMA GROWTH IN L349A AT 5 JOULES



(SAME SCALE AS PHOTOGRAPH)

Lamp L349A 10 Joules  
Arc Growth Sequence

4004

FIGURE 15 PLASMA GROWTH IN L349A AT 10 JOULES

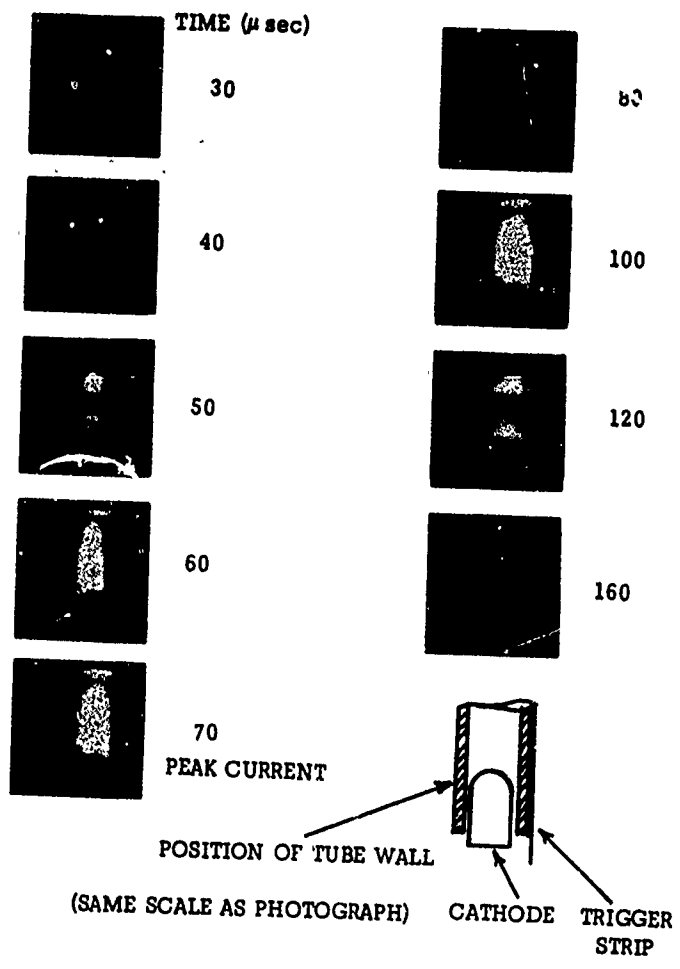


FIGURE 16 PLASMA GROWTH IN L349A AT 10 JOULES NEAR CATHODE

4005

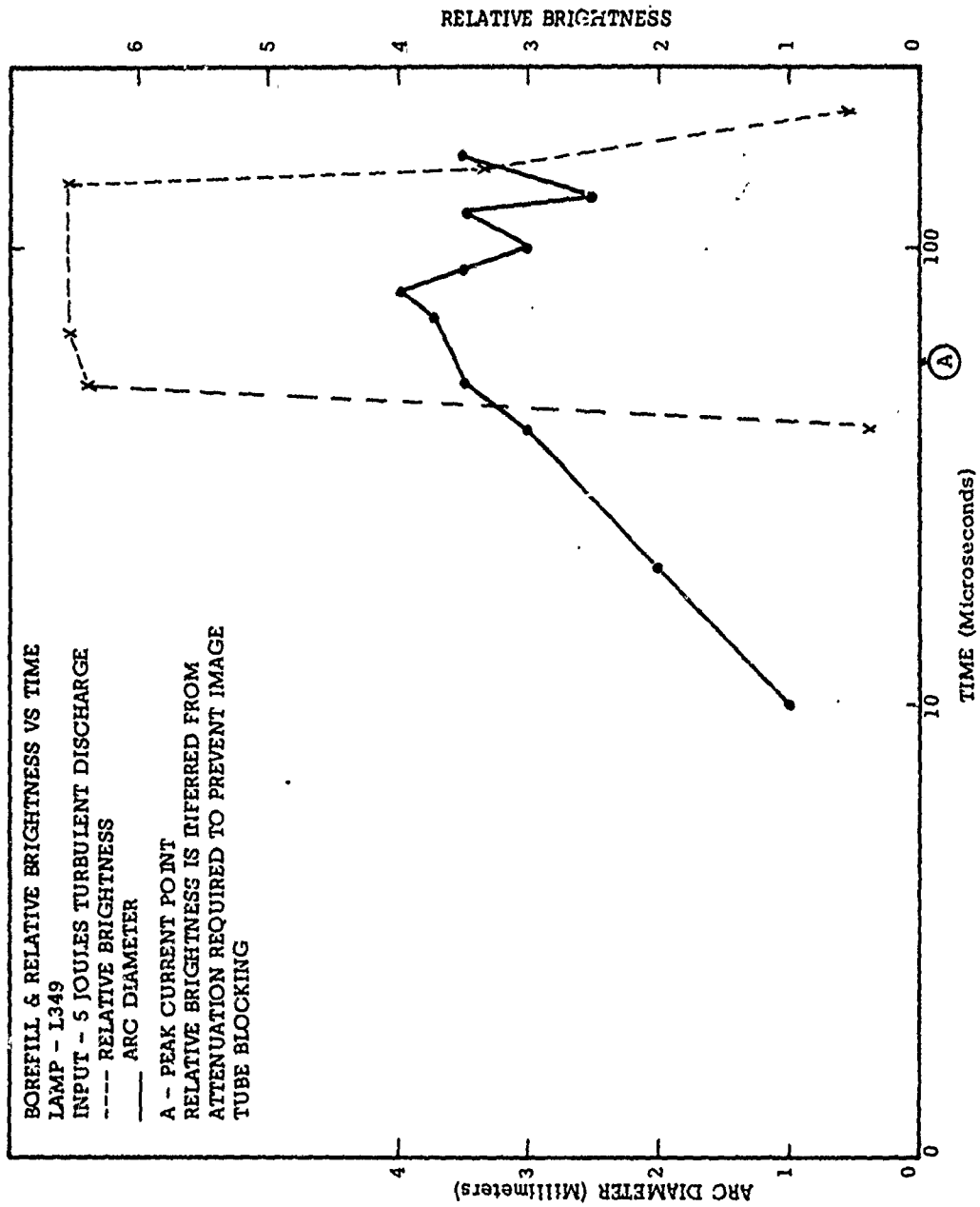


FIGURE 17 PLASMA DIAMETER IN 1.349 AT 5 JOULES

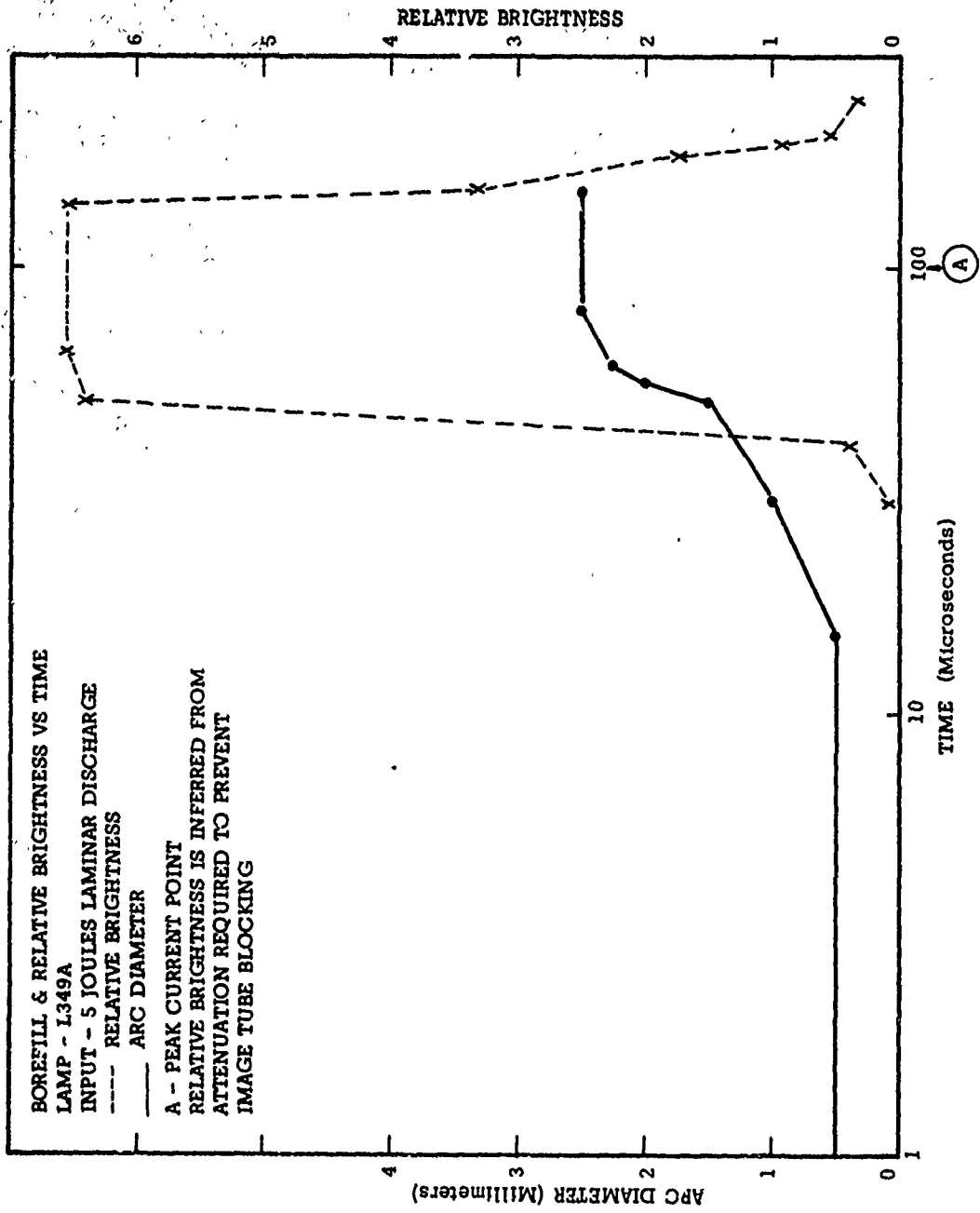


FIGURE 18 PLASMA DIAMETER IN L349A AT 5 JOULES

4006

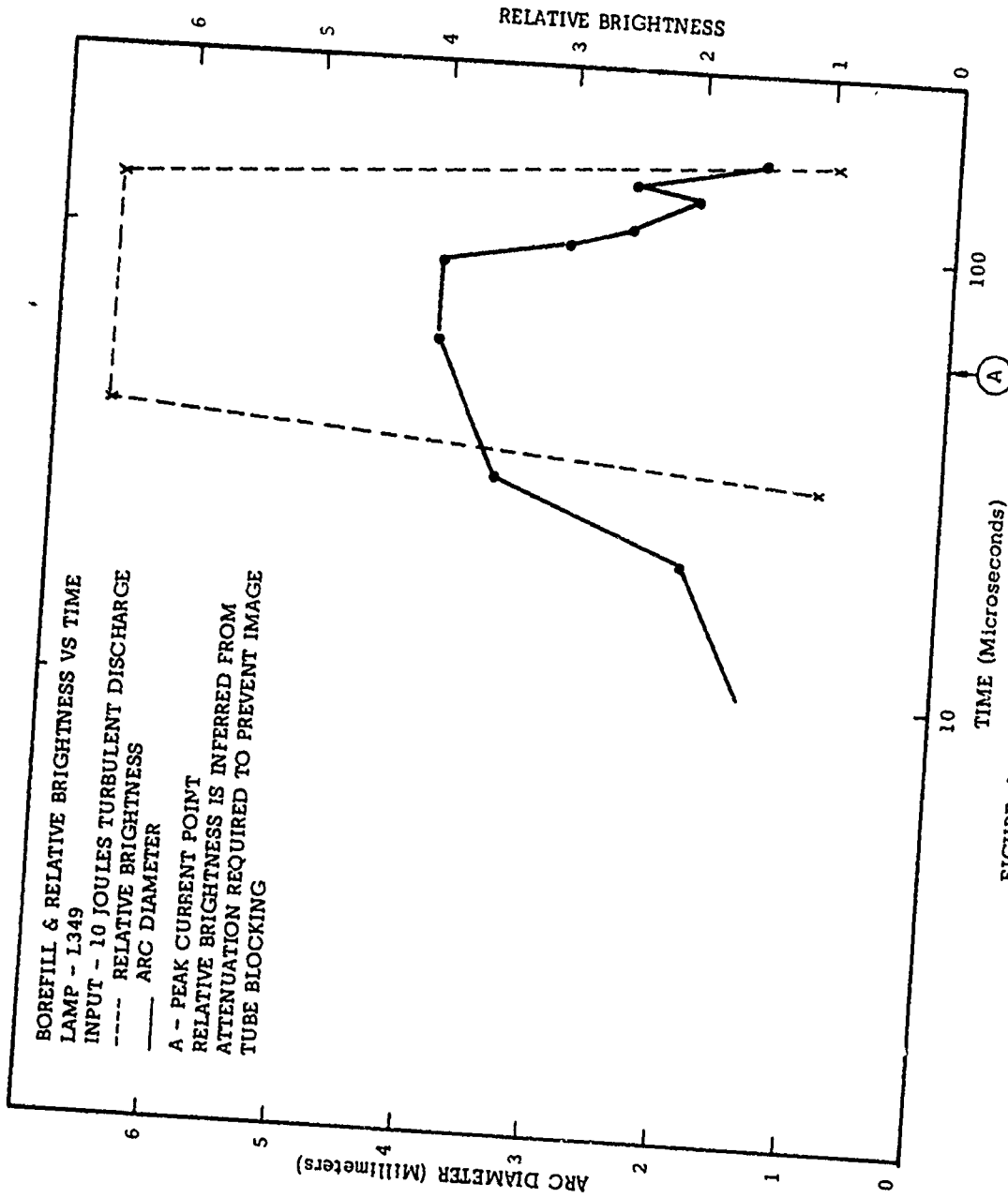


FIGURE 19 PLASMA DIAMETER IN L349 AT 10 JOULES

4007

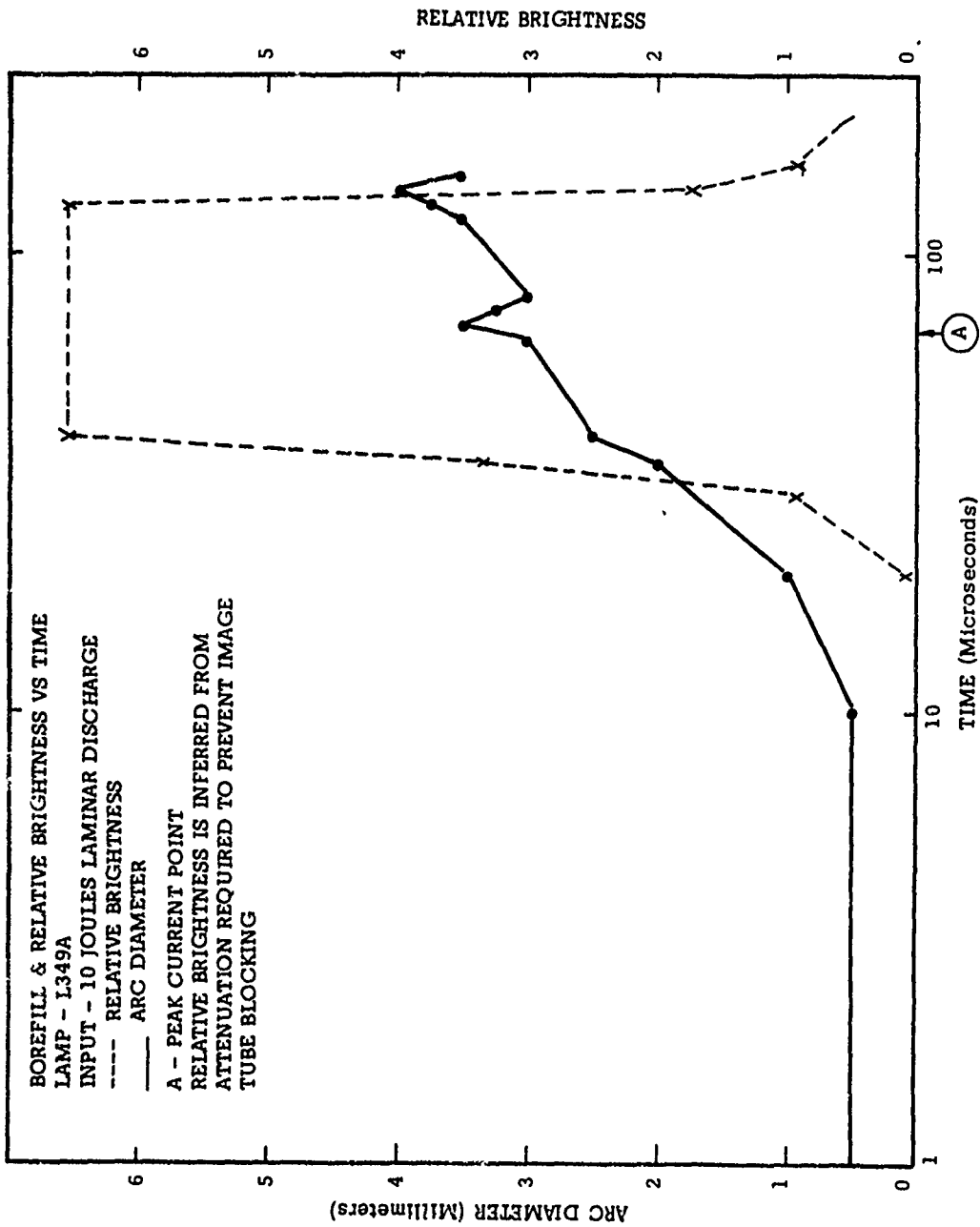


FIGURE 20 PLASMA DIAMETER IN L349A AT 10 JOULES

4008

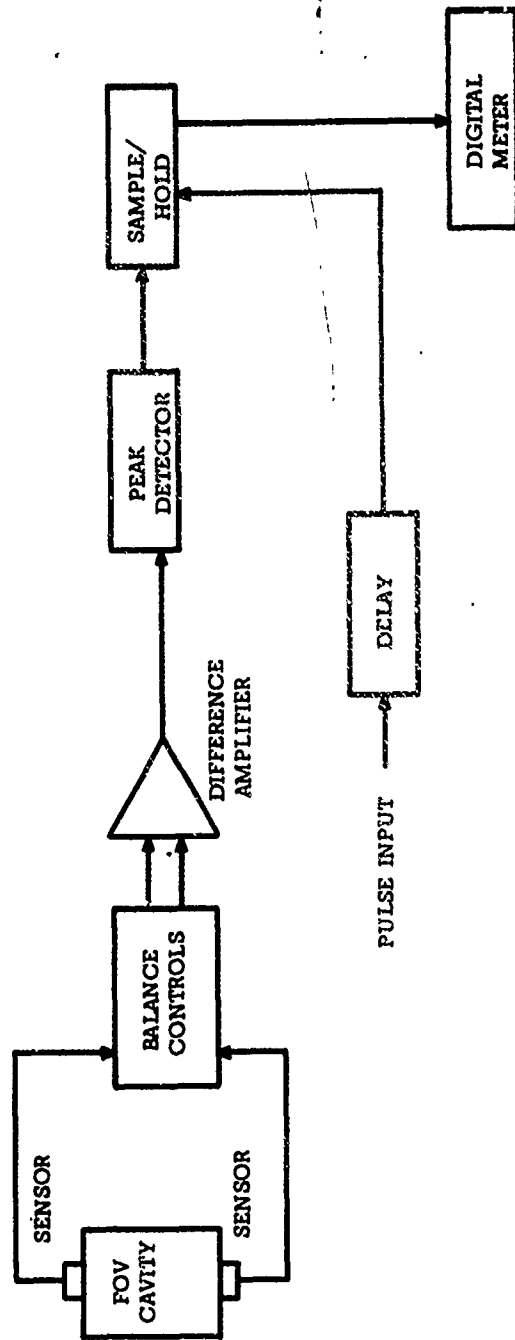


FIGURE 21 SCHEMATIC DIAGRAM OF PULSED FLUORESCENT ANALYSIS TESTER WITH DIGITAL READOUT ATTACHMENT.

4009

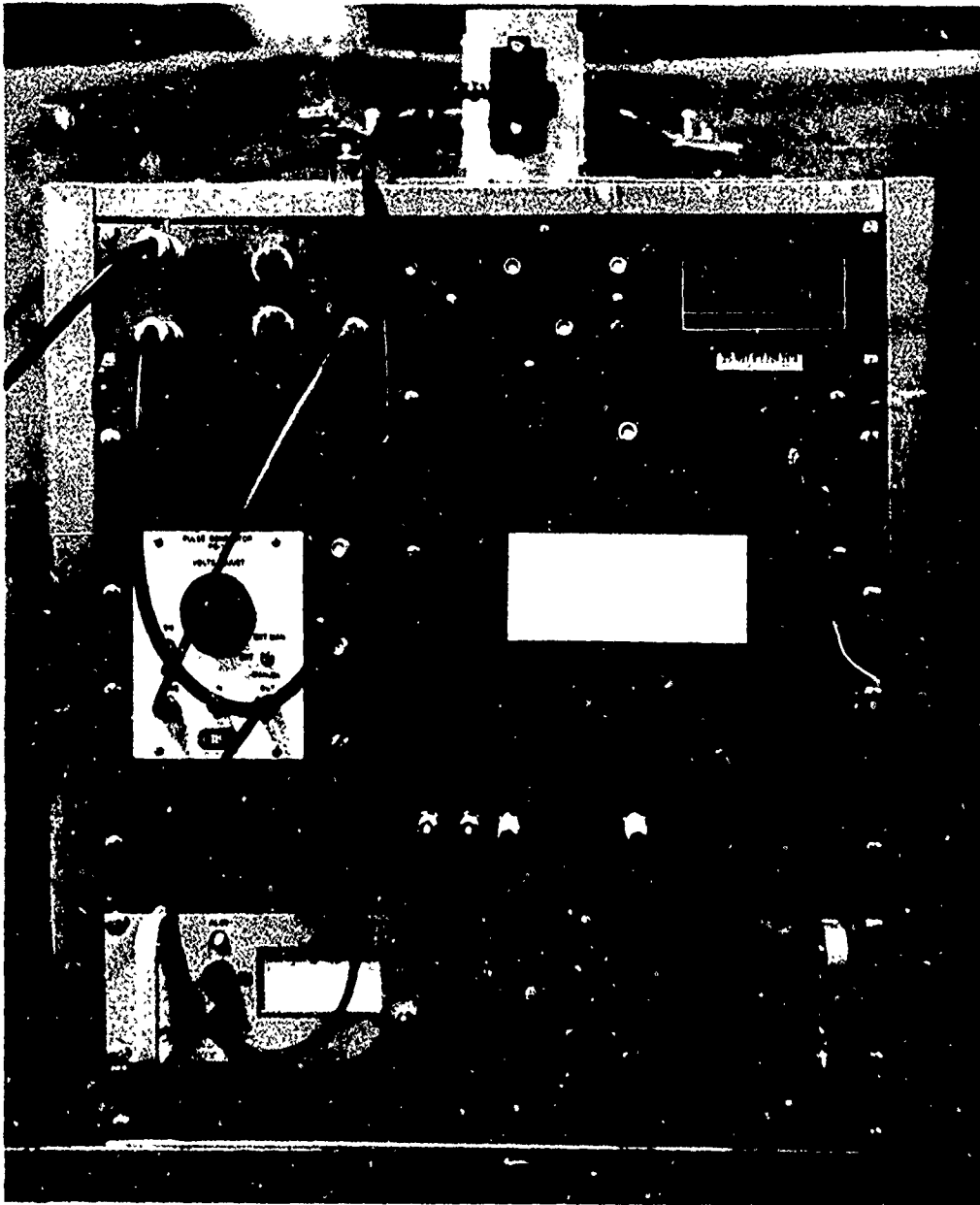


FIGURE 22 PHOTOGRAPH OF PULSED FLUORESCENT ANALYSIS TESTER WITH  
DIGITAL READOUT ATTACHMENT

4010

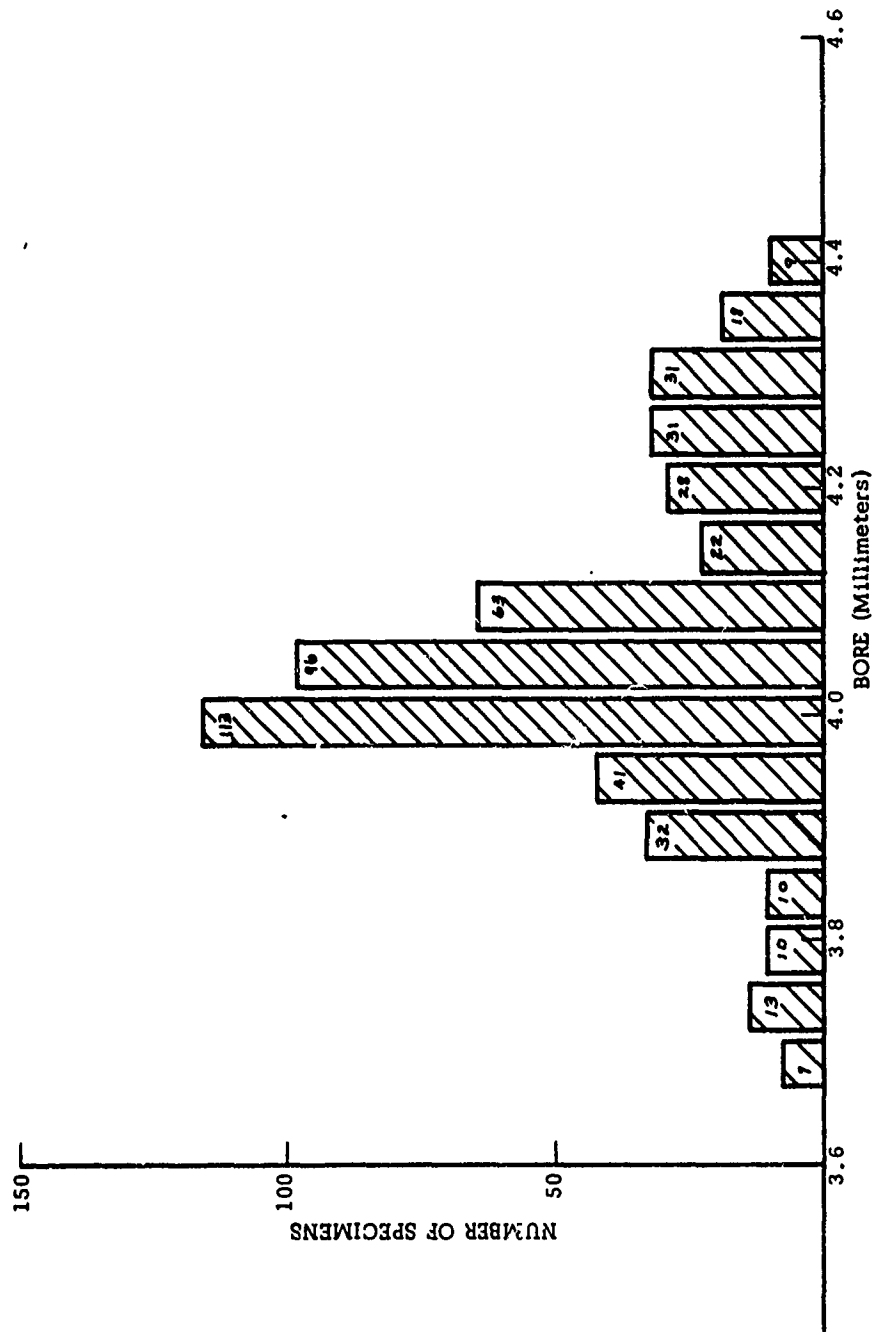


FIGURE 23 BORE SIZE DISTRIBUTION ON 4 X 6 MM AMERSIL QUARTZ TUBING FREQUENCY BAR CHART

40 11

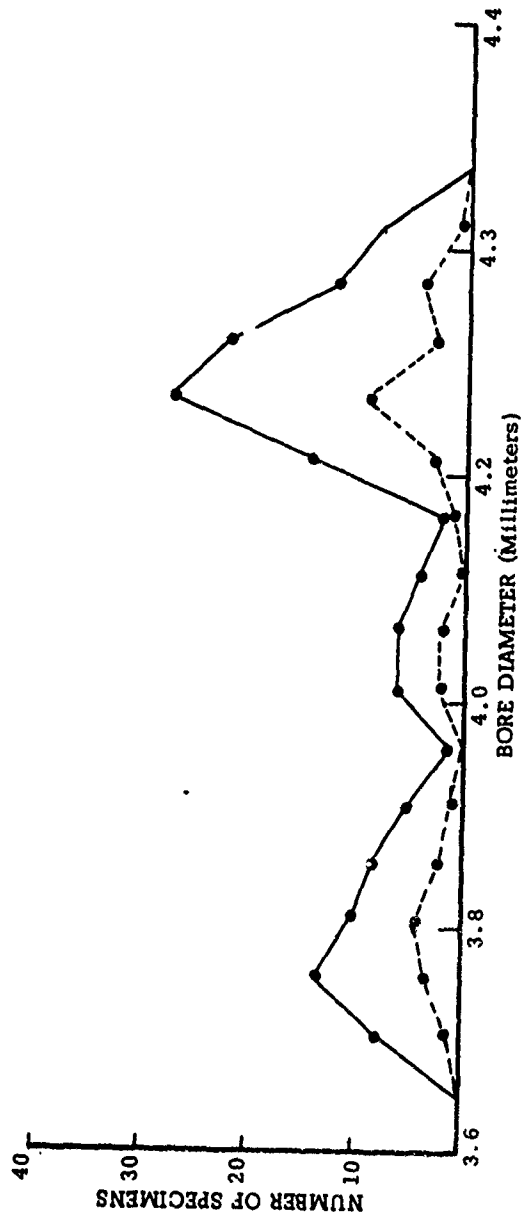


FIGURE 24 BORE SIZE DISTRIBUTION ON GERMISIL QUARTZ TUBING, FREQUENCY POLYGON

4012